MULTISCALE MODELING OF EBOLA TRANSMISSION DYNAMICS WITH TREATMENT

Duncan Otieno Oganga

A Thesis submitted to the School of Natural Sciences in partial fulfillment of the requirements for the award of the Degree of Doctor of Philosophy in Applied Mathematics of Masinde Muliro University of Science and Technology

March, 2021

DECLARATION

This research is my original work prepared with no other than the indicated sources and support and has not been presented elsewhere for a degree or any other award.

Signature..... Date .....

Duncan Otieno Oganga

SEA/H/01/14

CERTIFICATION

The undersigned certify that they have read and hereby recommend for acceptance of Masinde Muliro University of Science and Technology a research thesis entitled **'Multiscale Modeling of Ebola Transmission Dynamics with Treatment'**.

Signature..... Date.....

Dr. George O. Lawi

Department of Mathematics

Masinde Muliro University of Science and Technology.

Signature..... Date.....

Dr. Colleta A. Okaka

Department of Mathematics

Masinde Muliro University of Science and Technology.

COPYRIGHT

DEDICATION

This work is dedicated to my loving wife Sharon, Son Samuel and Daughters Purity and Emerald.

ACKNOWLEDGMENTS

I would like to begin by acknowledging GOD ALMIGHTY for helping me through upto this level. My sincere appreciation goes to my first supervisor Dr. George Lawi. You have been a great inspiration to me and to many others. Thank you so much for the sacrifice of time, knowledge, sleep and even resources that you put in to make this study successful. I also appreciate my second supervisor Dr. Colleta Okaka for the inputs that made this work to be completed well. Thank you so much. I also acknowledge Dr. Frankline Tireito, Dr. David Angwenyi, Dr. Michael Ojiema and Mr. Charles Wachira for their invaluable inputs in this work. I cannot forget my colleagues in Mathematics Department (MMUST), led by our able Chairperson Dr. Joyce Kagendo. Your encouragements and advice kept me going on and on until I have achieved this milestone. Thank you very much. I am also grateful to NRF team who gave me a grant that has supported part of this study. Last but not least, I thank my dear wife Sharon and my lovely children Samuel, Purity and Emerald for the understanding and unwavering support they gave me throughout these studies. Thank you all and may GOD bless you abundantly.

ABSTRACT

Ebola Virus Disease, (EVD) is a rare and deadly disease with high fatality rates in humans and other primates. It is introduced into the human population through direct contact with the infected hosts which include porcupines, fruit bats, chimpanzees, gorillas, monkeys and forest antelopes. Transmission from one human being to another takes place via direct contact with body fluids of the infected or indirectly via surfaces contaminated by these fluids. Mathematical models have been developed describing between host and within host dynamics of EVD separately. The within host models of EVD have considered mass action incidence rate which does not capture the effect of saturation due to high concentration of Ebola virions. As a result, a within host model incorporating saturated incidence rate and treatment has been developed and analysed. Stability analyses of the model developed show that the Infection Free Equilibrium (IFE) is locally and globally asymptotically stable, if $R_0^w < 1$, and when $R_0^w > 1$, an Endemic Equilibrium (EE) emerges, which is unique and globally asymptotically stable. The effect of treatment has been illustrated using numerical simulations. One of the control strategies of EVD is vaccination. The between host models of EVD incorporating vaccination available in literature assume that the vaccines grant full immunity. This may not be the case since the vaccines are still under development. Consequently, this study has developed and analysed a Susceptible Exposed Infected Recovered (SEIR) model incorporating an imperfect vaccine. Analyses of its equilibrium points have shown that if the basic reproduction number , $R_0^B < 1$, the disease dies out and if $R_0^B > 1$, the disease persists in the population. The impact of vaccination on the disease has also been established. Even though separate models have been used to study immunological and epidemiological dynamics of EVD, studies have shown that for virus infections, the infectivity of the host is directly proportional to the viral load. This therefore calls for the use of a multiscale model to capture this interdependence between scales. Multiscale models of EVD exist. However, they have not considered uninfected cells and infected cells, yet they are major players in the within host dynamics of EVD. This study therefore has formulated a multiscale model of EVD incorporating the uninfected cells, infected cells and the Ebola virions. Analyses of the Disease Free Equilibrium (DFE) and the EE show that the disease dies out if the basic reproduction number $R_0^c < 1$ and persists in the population when $R_0^c > 1$ respectively. Sensitivity analysis shows that the rate and efficacy of vaccination are the most sensitive parameters. This indicates that effort should be directed towards implementing an effective vaccination strategy to control the spread of the disease. It has also been established through simulations that when treatment efficacy is scaled up, the viral load goes down within a host and consequently, the transmission between hosts is also reduced. The models developed and analysed in this study have a significant impact on the control of EVD.

TABLE OF CONTENTS

DECLARATION ii

COPYRIGHT iii

DEDICATION iv

ACKNOWLEDGMENTS v

ABSTRACT vi

TABLE OF CONTENTS vii

LIST OF TABLES x

LIST OF FIGURES xi

LIST OF ABBREVIATIONS xii

CHAPTER ONE: INTRODUCTION **1**

1.1 Background information 1

1.2 Statement of the problem 4

1.3 Objectives of the study 5

1.3.1 Main objective 5

1.3.2 Specific objectives 5

1.4 Justification of the study 5

1.5 Significance of the study 6

1.6 Methods of the study 6

CHAPTER TWO: LITERATURE REVIEW **8**

2.1 Introduction 8

2.2 Within host models for Ebola 8

2.3 Between-host models for Ebola 10

2.4 Multiscale models 13

CHAPTER THREE: WITHIN HOST EBOLA MODEL **19**

3.1 Introduction 19

3.2 Model Formulation 19

3.3 Positivity and Boundedness of solutions 21

3.4 The Infection Free Equilibrium 22

3.4.1 Evaluation of the Basic Reproduction number, (R_0^w) 22

3.4.2 Local Stability Analysis of the Infection Free Equilibrium 24

3.5 Global Stability Analysis of the Infection Free Equilibrium 25

3.6 The endemic equilibrium point 26

3.6.1 Existence of the endemic equilibrium point 27

3.6.2 Stability analysis of the endemic equilibrium point 28

3.7 Numerical Simulations and Discussions 31

CHAPTER FOUR: BETWEEN HOST EBOLA MODEL **35**

4.1 Introduction 35

4.2 Assumptions in the model 35

4.3 Description and Formulation of the model 35

4.4 Positivity and Boundedness of Solutions 37

4.5 The Disease Free Equilibrium 38

4.6 The Basic Reproduction number 38

4.7 Stability Analysis of the Disease Free Equilibrium 39

4.7.1 Local Stability Analysis 39

4.7.2 Global Stability Analysis of the Disease Free Equilibrium 40

4.8 The Endemic Equilibrium 41

4.8.1 Existence of the Endemic Equilibrium 41

4.8.2 Local Stability Analysis of the Endemic Equilibrium 42

4.8.3 Global Stability Analysis of the Endemic Equilibrium 43

4.9 Numerical Simulation and Discussion 47

CHAPTER FIVE: MULTISCALE EBOLA MODEL **51**

5.1 Introduction 51

5.2 Within Host Model 51

5.3 Between Host Model 52

5.4 Multiscale Model 52

5.5 Reproduction number 53

5.6 Local Stability Analysis of the Disease Free Equilibrium 54

5.7 Global Stability Analysis of the Disease Free Equilibrium 55

5.8 Existence of the Endemic Equilibrium 55

5.9 Local Stability Analysis of the Endemic Equilibrium 56

5.10 Global Stability Analysis of the Endemic Equilibrium 57

5.11 Sensitivity Analysis 58

5.12 Numerical Simulation and Discussion 60

CHAPTER SIX: CONCLUSIONS AND RECOMMENDATIONS **63**

6.1 Conclusions 63

6.2 Recommendations 64

REFERENCES **65**

APPENDICES **71**

0.1 Codes used in simulating within host model 71

0.2 Direction fields of IFE 72

0.3 Between host model 73

0.4 Multiscale model 74

List of Tables

3.1 Description of Parameters and Variables 21

3.2 **Values of parameters** 31

4.1 Parameters and Variables of Model (4.1) 36

4.2 **Parameter Estimates for the Model** 47

5.1 Sensitivity indices 59

5.2 **Values of the parameters in the model** 60

List of Figures

3.1 Within host Model Flow Chart 20

3.2 Stability of IFE 31

3.3 Effect of varying ρ on Evolution of Target cells 32

3.4 Effect of varying ρ on Evolution of Virions 33

3.5 Effect of varying ρ on Evolution of Infected cells 33

4.1 Flow Diagram of Model (4.1) 36

4.2 Evolution of State variables without intervention 47

4.3 Evolution of Susceptible Individuals with varying efficacy of vaccine 48

4.4 Evolution of Infected Individuals with varying efficacy of vaccine 49

4.5 Dynamics between Infected and Exposed individuals 50

5.1 Flow Diagram of the Multiscale Model 52

5.2 The stability of DFE 60

5.3 Effect of number of Virions on Infected individuals 61

5.4 Effect of ω on Infected individuals with time 62

LIST OF ABBREVIATIONS

EVD	:	Ebola Virus Disease
SIR	:	Susceptible Infected Recovered
EVD	:	Susceptible Exposed Infected Recovered
DRC	:	Democratic Republic of Congo
IFE	:	Infection Free Equilibrium
DFE	:	Disease Free Equilibrium
EE	:	Endemic Equilibrium
SIRS	:	Susceptible-Infective-Recovered-Susceptible
MATLAB	:	Mathematics Laboratory
ODEs	:	Ordinary Differential Equations
RVD	:	Rational Vaccine Design
PDE	:	Partial Differential Equation
WHO	:	World Health Organization

CHAPTER ONE

INTRODUCTION

1.1 Background information

Ebola Virus Disease, (EVD) is a deadly disease with high fatality rates in humans and primates [41]. The first cases were reported in 1976 in Democratic Republic of Congo (DRC) and in Sudan. Since then, there have been several outbreaks which have been documented, the largest being the one that occured in West Africa in Sierra Leone, Guinea and Liberia in 2014 [4]. As at December 2014, 4656 deaths from this largest EVD outbreak had been reported by World Health Organisation (WHO), with most cases occuring in Liberia [15]. At this moment, there is an ongoing infection of EVD in DRC in the regions of Ituri and North Kivu provinces. It began in August 2018. By end of August 2019, about 3000 cases and 2000 deaths had been reported [26] and according to WHO , by 16^{th} June 2020, cases were 3,463, survivors were 1,171 and deaths were 2,280 . Records show that this current outbreak is the largest ever recorded in DRC and the second largest outbreak in the world. The Director General of WHO declared it a Public Health Event of International Concern (PHEIC) on 17th July 2019 by the WHO [14].

EVD is introduced into the human population through direct contact with the infected hosts which include porcupines, fruit bats, chimpanzees, gorillas, monkeys and forest antelopes. Transmission from one human being to another takes place via direct contact with body fluids of the infected or indirectly via surfaces contaminated by these fluids [45]. Once exposed to the virus, the patient become symptomatic within 2 to 21 days. The symptoms of EVD include abdominal pain, diarrhea, fever, malaise, sore throat and asthenia. Once the patient becomes symptomatic, it takes about 10 days for hemorrhagic manifestations to occur. This leads to death in 50 to 90% of patients [4].

Currently, there is no licenced antiviral drug treatment for the Disease. However, clinical trials are going on for several antiviral drugs. For instance, there is a multidrug clinical trial of Ebola therapies that began in November 2018 and is ongoing in DRC. The therapies comprise three different antibody treatments (mAb114, REGN- EB3 and ZMapp) and one antiviral drug (Remdesivir or GS- 5734) [1]. Investigators are hopeful that the trial will provide critical information on which treatments are most effective at treating Ebola [44]. Results show that EVD patients receiving either of the first two antibody treatments, i.e REGN-EB3 or mAb114 had a greater chance of survival compared with the other two [14]. Consequently, the U.S Food and Drug Administration (FDA) has given orphan drug status to these two most effective drugs and so should receive prompt review for licencing [26]. These drugs have antibodies that gets attached onto the virus and thus hampering its replication inside the host's body. They also trigger the body's immune system to kill the infected cells; thus lowering the viral load. Apart from the clinical trials of the drug therapies, EVD patients usually receive supportive care which comprises providing fluids and electrolytes (body salts), managing fever and pain, maintaining oxygen status, reducing vomiting and diarrhea and treating other infections, if they occur [8]. These in turn boosts the immune system.

Up to now,there is only one vaccine, (rVSV-ZEBOV) that has been approved for use by the U.S. FDA [8]. This vaccine has been tested in the ongoing outbreak in DRC using ring vaccination strategy and its efficacy was found to be 97.5%. From these tests, it was also realised that even those people who are already infected at the time of vaccination may have greater chances of survival [46]. This therefore calls for enhancement of treatment and vaccination as part of interventions in the control of EVD.

For most infectious diseases, two processes are involved in the host-pathogen interaction. One is the within host process at the individual level and the other one is the between host process which encompasses the disease transmission.

These processes can be modeled mathematically giving rise to within host models and between host models [51]. In mathematical modeling of within host processes of EVD, the modelers have used the mass action incidence rate to describe the interaction between target cells and Ebola virions. They assume that there is a bilinear interaction between these cells and virions. However, it is expected that when there is invasion in a host, the immune system always comes into play to prevent further infection. Moreover, a high concentration of Ebola virions leads to saturation effect. These may trigger nonlinear responses. One of the control strategies of EVD is vaccination of the susceptible individuals. It has been assumed in the between host models of EVD incorporating vaccination that the vaccine grants full immunity [6]. However, the Ebola vaccines are still under development and so it may be safer to assume that the efficacy of the vaccine varies.

Single scale models describing dynamics of diseases exist. Despite these extensive studies, the outbreak of some diseases, (including EVD) cannot still be predicted. This unpredictability may be attributed to the fact that these models are single scale yet disease dynamics are multiscale in nature [33]. In the recent past, efforts have been directed towards multiscale models linking these two separate scales. The resulting multiscale models have the capacity to uncover new insights into infectious diseases [3]. For instance, multiscale models of HIV and AIDS have been used to evaluate the effect of the within host parameters on the between host reproduction number, prevalence of the disease among other things. Multiscale models of EVD exist in literature [31],[2]. However, these studies have only considered viral dynamics and antibodies, leaving out other cells within a host such as the target cells which are very important in EVD dynamics.

1.2 Statement of the problem

The within host models of Ebola Virus Disease, (EVD) studied so far have considered the mass action incidence rate which assumes that the rate of infection is bilinear in both uninfected cells and Ebola virions. However, it is expected that a nonlinear response may occur at high concentration of Ebola virions due to the saturation effect. The behavior change, normally associated with the saturated incidence term may be considered as being analogous to the immune response. Thus, a saturated incidence rate is more appropriate for the viral and target cell interaction. Some of the between host models of EVD studied have considered vaccinating a proportion of the susceptible individuals as an effective tool of combating this disease. These models assume full protection against EVD which may not be the case since the vaccines are still under development. Even though separate models have been used to study immunological and epidemiological dynamics of EVD, studies have shown that for virus infections such as HIV and AIDS, EVD among others, the infectivity of the host is directly proportional to the viral load [2]. This therefore calls for the use of a multiscale model to capture this interdependence between scales. The multiscale models of EVD that are available in literature $\Big($see [31],[2]$\Big)$ have not explicitly modeled the interaction between uninfected cells and the virions. This interaction is important since it produces infected cells which in turn produce Ebola virions.

1.3 Objectives of the study

1.3.1 Main objective

The main objective of this study is to develop and analyze a multiscale model for Ebola transmission dynamics with treatment.

1.3.2 Specific objectives

The specific objectives of this study are;

(i) To develop a within host model for Ebola Virus Disease with a saturated incidence term and analyze its long term solutions.

(ii) To develop a between host model for Ebola Virus Disease incorporating an imperfect vaccine and analyze its long term solutions.

(iii) To couple the within and between host models developed and analyze the resulting multiscale model.

(iv) To evaluate the role of treatment as a control strategy.

1.4 Justification of the study

Ebola is an emerging threat of Public Health in Africa. The high fatality and the continuous high risk faced by frontline healthcare workers makes it an important nosocomial infection. Despite the advancements in studying mathematical models of EVD, the outbreaks of the disease remains unpredictable. This may be due to the fact that most models describe the dynamics of EVD in a single scale. In reality, almost all problems (including diseases) have multiple scales. Therefore there is need for multiscale modeling of EVD.

1.5 Significance of the study

Multiscale modeling of Ebola is important in understanding the interdependence of scales. This study has also incorporated the efficacy of treatment in the within host model. This has helped evaluate the role of treatment on Ebola transmission dynamics. The novel results of the analysis of the models developed are helpful to policy makers and health practitioners in coming up with effective control strategies.

This study also contributes knowledge in Mathematics since multiscale modeling in a very active area of research.

1.6 Methods of the study

The following methods have been used in this study.

(a) **Ordinary Differential Equations (ODEs)**.

All the models developed and analyzed have been described by a system of ODEs.

The first model describes the within host dynamics. It has uninfected cells , infected cells and the free virus particles represented by $X(t)$, $Y(t)$ and $L(t)$ respectively . The uninfected cells grow in a logistic manner and a saturated force of infection has been adopted. The uninfected cells are taken to have logistic growth since their number is bounded.

Treatment has been incorporated in this model. One of the proposed treatment for EVD is convalescent blood transfusion. It was used during the 1995 Kikwit Ebola Outbreak in treating 8 infected individuals. After the treatment, it was reported that only 1 patient died [49]. Trials for several drug therapies are ongoing at the moment. In this study, the efficacy of treatment is given by ρ.

For the between host model, the population is subdivided into the Susceptible $S(t)$, the Exposed $E(t)$, the Infected $I(t)$ and the recovered $R(t)$.

Evidence show that people who have recovered from EVD had antibodies that could be detected after 10 years [8] and therefore we consider recovery as confering temporary immunity.

The bridge of within to between host is by considering transmission in the between host model as a saturated function of the viral load of the within host level.

(b) **Stability analysis**.

Given a dynamical system, a vector $\bar{x}$ is considered to be its equilibrium point if it satisfies the property that once the system state vector is equal to $\bar{x}$, it remains equal to $\bar{x}$ for all time.

The stability of a dynamical system is defined with respect to its equilibrium point. An equilibrium point is stable if when the state vector is given a small perturbation, it tends to return to it [11].

To determine the stability of a given equilibrium point, the basic reproduction number is used. For instance, for the case of DFE, when it is greater than 1, the DFE is unstable and when it is less than 1, this equilibrium is stable and we predict that the pathogen will be cleared [17]. The Basic reproduction numbers of each model has been calculated.

The equilibrium points of the models have been found and each model has been linearized by finding the Jacobian. Local and global stability of each model has been analyzed using variety of techniques namely Routh Hurwitz method, Center Manifold Theorem, Descartes Rule, Geometric Approach, Comparison method and Lyapunov method.

(c) **Numerical Simulations**.

The long term behavior of the solutions have been determined through numerical simulations using MATLAB software.

CHAPTER TWO

LITERATURE REVIEW

2.1 Introduction

Mathematical models are built on basic assumptions usually with a view to estimating the necessary intervention strategies [47]. Below is a survey of some mathematial models for Ebola Virus Disease and some models for other diseases useful in this study.

2.2 Within host models for Ebola

These are models representing the dynamics of a disease within an individual [27].One of the early within host models, regarded as the standard model for modeling virus reproduction was used in [32] and in [35] to model the within host dynamics of HIV. It is given below.

$$\begin{aligned} \frac{dX(t)}{dt} &= \lambda - dX(t) - \beta X(t)V(t), \\ \frac{dY(t)}{dt} &= \beta X(t)V(t) - aY(t), \\ \frac{dV}{dt} &= kY(t) - uV(t) \end{aligned} \tag{2.1}$$

where $X(t), Y(t), V(t)$ represent target (cytotoxic T) cells, infected cells, virus particles respectively.

Within host studies and mathematical models of Ebola exist in literature. Some of these are discussed below;

Vincent *et.al* [43] designed an experiment where they infected 20 mice with ebola virus. They treated some with favipiravir and left some untreated. They then characterised their viral dynamics. Their model showed that the drug effectively blocks viral production with antiviral effectiveness reaching up to 99.6%. From this experiment, they concluded that favipiravir should be administered as early as possible for it to be effective.

Sophia *et. al* [37] developed an immunological model to explore the immune response to EBOV and to assess the effect of vaccination at the cellular level. In this work, they used Herz model to analyse EBOV dynamics within an individual and used Tuckwell model to analyse the immune response. These models provided information about the workings of the immune system and provided thresholds for parameters. They concluded from their results that the vaccinated cytotoxic T lymphocyte response contained the EBOV growth.

Thomas *et.al* [39] developed and analysed a within host model describing EBOV dynamics. The model is given by the following system of nonlinear ODEs

$$\begin{aligned}
\frac{dX(t)}{dt} &= \lambda - \beta V(t)X(t) - \mu X(t), \\
\frac{dI(t)}{dt} &= \beta V(t)X(t) - \rho I(t)T(t) - \alpha I(t), \\
\frac{dV(t)}{dt} &= cI(t) - \gamma V(t), \\
\frac{dT(t)}{dt} &= \rho I(t)T(t) - \delta T(t)
\end{aligned} \tag{2.2}$$

where $X(t), I(t), V(t), T(t)$ represent uninfected cells, infected cells, EBOV particles and cytotoxic T cells respectively. They used this model to examine the course of ebola infection within the immune system in a human being. They came up with two threshold parameters namely: the viral reproduction number, denoted by R_0 and the immune response number, denoted by R_1. These two threshold parameters were used to predict the local asymptotic stability of the system around the equilibrium points.

Lasisi *et.al* [22] improved the model (2.2) by introducing the drug usage. Their model is

$$\begin{aligned}
\frac{dU(t)}{dt} &= \beta - \mu_1 U(t) - (1-\phi)\alpha U(t)V(t), \\
\frac{dI(t)}{dt} &= (1-\phi)\alpha U(t)V(t) - \mu_2 I(t) - \delta_1 I(t)T(t), \\
\frac{dV(t)}{dt} &= \omega I(t) - \mu_3 V(t) - \delta_2 B(t)V(t), \\
\frac{dT(t)}{dt} &= k_1 T(t) + \gamma I(t)T(t) - \mu_4 T(t), \\
\frac{dB(t)}{dt} &= k_2 B(t) + \theta B(t)V(t) - \mu_5 B(t)
\end{aligned} \tag{2.3}$$

where ϕ is the efficacy of drug, $U(t)$ is the number of uninfected cells, $I(t)$, the number of infected cells, $V(t)$ the number of free virions, T, the number of cytotoxic T lymphocytes and B is the number of B cells (antibodies). In the analysis and simulations of this model, it was shown that the efficacy of drug usage has an effect on the number of free virions. This in turn affects the number of infected cells.

In the Herz model, Tuckwell model and models (2.2)and (2.3), mass action incidence rate has been used. In mass action, it is assumed that the infection rate is strictly linear in the entire range of the uninfected cells and Ebola virions. This may not be realistic since factors such as saturation and immune response can cause a nonlinear interaction [36].

2.3 Between-host models for Ebola

Navjot *et.al* [30] developed and analyzed a general SIRS epidemic model. They incorporate the effects of media awareness on the transmission of infectious diseases. From their analysis, they reported that media programs that create awareness about a particular disease have positive impact on reducing disease prevalence in a given region of interest. This shows that mathematical models can be used to evaluate the impact of a given intervention on the dynamics of a disease.

Sylvie [38] developed, analysed and numerically simulated a mathematical model for EVD. She used the model to investigate the effect of media campaigns on the transmission of the disease. Through simulations, she showed that media has a beneficial effect in reduction of the EVD cases. She recommended the spacing out of the media campaigns in intervals of time for more effectiveness.

Amira and Delfim [5] developed and analysed an SEIR model for EVD to be used in predicting and controlling the disease. The model is given below

$$\begin{aligned}
\frac{dS(t)}{dt} &= -\beta S(t)I(t), \\
\frac{dE(t)}{dt} &= \beta S(t)I(t) - \gamma E(t), \\
\frac{dI(t)}{dt} &= \gamma E(t) - \mu I(t), \\
\frac{dR(t)}{dt} &= \mu I(t)
\end{aligned} \tag{2.4}$$

However, model (2.4) does not include deaths caused by the disease. This is not realistic since EVD leads to death in 50 to 90% of infections as stated earlier. In addition, it does not include vital dynamics like births and natural deaths yet they affect the size of the four classes of population.

Ellina and Evgenii [15] improved the model (2.4) as given below.

$$\begin{aligned}
\frac{dS(t)}{dt} &= -\frac{\Big(\beta I(t) + \alpha E(t)\Big)S(t)}{N}, \\
\frac{dE(t)}{dt} &= \frac{\Big(\beta I(t) + \alpha E(t)\Big)S(t)}{N} - \sigma E(t), \\
\frac{dI(t)}{dt} &= \sigma E(t) - \gamma I(t), \\
\frac{dR(t)}{dt} &= \gamma I(t)
\end{aligned} \tag{2.5}$$

They considered population with a constant size N and two infection routes through the exposed individuals and the infected individuals. This study, however, did not consider births, natural deaths and disease induced deaths. It has also been documented that the exposed individuals do not transmit EVD [9].

Wetere *et.al* [40] developed an SIRD model of EVD incorporating quarantine and vaccination as control strategies.

The model is given below.

$$\begin{aligned}
\frac{dS(t)}{dt} &= \gamma R(t) - \frac{\beta(1-q)S(t)I(t)}{N(t)} - vS(t), \\
\frac{dI(t)}{dt} &= \frac{\beta(1-q)S(t)I(t)}{N(t)} - \alpha_1 qI(t) - \alpha_2(1-q)I(t) - \delta_1 I(t) - \delta_2 I(t), \\
\frac{dR(t)}{dt} &= \alpha_1 qI(t) + \alpha_2(1-q)I(t) + vS(t) - \gamma R(t), \\
\frac{dD(t)}{dt} &= \delta_1 I(t) + \delta_2 I(t)
\end{aligned} \tag{2.6}$$

where N(t) is the total population, γ is the rate of loss of infection acquired immunity, β is the contact rate, q is the rate of quarantine, v is the vaccination rate, α_1 and α_2 are recovery rates while δ_1 and δ_2 are death rates. Through numerical simulations, it has been shown that quarantine and vaccination are effective interventions against EVD.

Amira and Delfim [6] also improved their model (2.4) by introducing vital dynamics and vaccination. The improved model is given below.

$$\begin{aligned}
\frac{dS(t)}{dt} &= \delta N - \beta S(t)I(t) - \lambda S(t) - uS(t), \\
\frac{dE(t)}{dt} &= \beta S(t)I(t) - \gamma E(t) - \lambda E(t), \\
\frac{dI(t)}{dt} &= \gamma E(t) - \mu I(t) - \lambda I(t), \\
\frac{dR(t)}{dt} &= \mu I(t) - \lambda R(t) + uS(t)
\end{aligned} \tag{2.7}$$

Model (2.6) and model (2.7) assumed that all who have been vaccinated are immune to infection. This may not be true since vaccines for EVD are still under development and trials.

2.4 Multiscale models

Multiscale models coupling between host and within host models for diseases including Ebola are available. Below is a survey of some multiscale models that scholars have developed and analysed.

Jie *et.al* [20] came up with an immunoepidemiological model of HIV and AIDS. They first introduced a within host model describing the within host dynamics of HIV and AIDS. Their between host model is age structured and they used it to describe the disease dynamics in the population. They then coupled the two models and formed an immunoepidemiological model. The coupling was done via the between host parameters that depend on viral load and the number of CD4+ T cells. They theoretically analyzed their mathematical models. Through simulations, they found out that there is interdependence between the two scales.

Winston *et.al* [48] developed a modeling framework that can be used in coupling the within and between host dynamics of a disease. They illustrated the working of this framework using human schistosomiasis. The pathogen causing this disease, i.e trematode worm has part of its dynamics in the environment, e.g contaminated water. Thus, the dynamics of the different scales were coupled via the environment. The resulting multiscale model was tested and found to be epidemiologically well posed. Through analysis, they established that there is a link between the within and between host scales via the environment.

Zhilan *et.al* [16] came up with a mathematical model used in linking the between and within host dynamics of a disease and used it as a multiscale model for Toxoplasma gondii. Part of the life cycle of this parasite is interaction with the environment. Their between host model is;

$$\begin{aligned} \frac{dS(t)}{dt} &= \mu N(t) - \lambda E(t)S(t) - \mu S(t), \\ \frac{dI(t)}{dt} &= \lambda E(t)S(t) - \mu I(t) \end{aligned} \tag{2.8}$$

Here, $E(t)$ denotes contamination level of the environment at any time. It depends on the parasite load $V(t)$ and the number of individuals who are infected, $I(t)$. Its equation is

$$\frac{dE(t)}{dt} = V(t)I(t)\theta(1 - E(t)) - \gamma E(t) \tag{2.9}$$

where θ denotes the rate of contamination and γ is the clearance rate. Their within host model is given below;

$$\begin{aligned} \frac{dT(t)}{dt} &= \Lambda - kV(t)T(t) - mT(t), \\ \frac{dT^*(t)}{dt} &= kV(t)T(t) - (m+d)T^*(t), \\ \frac{dV(t)}{dt} &= g(E) + pT^*(t) - cV(t) \end{aligned} \tag{2.10}$$

with T(t) denoting the density of susceptible cells, $T^*(t)$ denoting the density of the cells that are infected, k denotes the rate of infection of the susceptible cells, m is the natural mortality rate and d is the mortality rate of cells as a result of infection, p denotes the rate of reproduction of the parasite by a cell that is infected c denotes the mortality rate of parasites while $g(E)$ is the rate of inoculation of an average host. In this work, $g(E)$ has been used in linking the dynamics between the two scales. In their analysis, they realized that there is a dependence of the reproduction number of the between host model on the parameters of the within host model.

In the studies by Winston *et.al* [48] and Zhilan *et.al* [16], the two models are linked via an environmental component. This may not be applicable for multiscale modeling of EVD since there is no environmental component in the dynamics of EVD.

Alexis *et.al* [3] developed an immunoepidemiological mathematical model coupling an immunological model and an epidemiological model of disease. The immunological model is given as;

$$\begin{aligned} \frac{dV(t)}{dt} &= pV(t)(1-\frac{V(t)}{K_v}) - cvE(t)V(t), V(0) \geq 0, \\ \frac{dE(t)}{dt} &= (N_E - \delta_E E(t)) + G(V)E(t), E(0) \geq 0 \end{aligned} \tag{2.11}$$

Here, $V(t)$ is the number of free virions at time t, $E(t)$ denotes the population of T-Cells at time t, p is the rate of replication of the virions rate and K_v denotes the carrying capacity. They imposed the properties; $G(0) = 0$, $G'(V) = \frac{dG}{dV} > 0$ and considered a special case of G in the Michaelis-Menten form $G(V) = \frac{rV}{V+K_E}$ in the analysis.

In this model, T- cells get replenished at the rate N_E and they are cleared at the rate δ_E. The virus is cleared at the rate cv while r_V is the maximum value of the virions and K_E is half saturation constant.

Their between host model is;

$$\begin{aligned} \frac{dS(t)}{dt} &= (N_S - \delta_S S(t)) - \beta S(t)I(t), S(0) > 0, \\ \frac{dI(t)}{dt} &= \beta S(t)I(t) - \delta_I I(t), I(0) \geq 0. \end{aligned} \tag{2.12}$$

Here, β is the transmission rate while δ_S and δ_I denote the mortality rate of susceptibles and infected individuals respectively. They coupled the two models using the viral load by considering the transmission between different people as a function of the viral load within an infected individual, i.e $\beta = \beta(V)$ where $\beta(0) = 0$ and $\beta'(V) > 0$.

Linear, logistic and saturation form of the coupling function were considered in the numerical analyses.

Their main result was the derivation of the between host model reproduction number as a general increasing function of the reproduction number of the within host model. This model may not be suitable to study EVD since the within host model considers the interaction between virions and the T cells yet T cells are not target cells in EVD dynamics.

Feng *et.al* [51] presented a mathematical model allowing the immunological and epidemiological processes to depend on one another. Their within host model is as given below;

$$\begin{aligned}
\frac{dT(t)}{dt} &= \Lambda_c - kT(t)V(t) - \mu_c T(t), \\
\frac{dT_*(t)}{dt} &= kT(t)V(t) - (\mu_c + \delta_c)T_*(t), \\
\frac{dV(t)}{dt} &= pT_*(t) - cV(t)
\end{aligned} \tag{2.13}$$

where $T(t)$ and $T_*(t)$ denotes the density of target host cells and infected host cells respectively and $V(t)$ denotes the viral load within a host.

The between host model that they used is given below;

$$\begin{aligned}
\frac{dS(t)}{dt} &= b(S,I) - \beta(V)S(t)I(t) - \mu S(t), \\
\frac{dI(t)}{dt} &= \beta(V)S(t)I(t) - \mu I(t)
\end{aligned} \tag{2.14}$$

Here, b(S,I) is the rate of recruitment of susceptible individuals, μ denotes the natural mortality rate and $\beta(V)$ denotes the transmission rate. This rate of transmission is taken to be directly proportional to the viral load, $V(t)$. The multiscale model that resulted from coupling these two sub models is given below.

$$\begin{aligned}
\frac{dS(t)}{dt} &= \Lambda - \beta S(t)V(t)I(t) - \mu S(t), \\
\frac{dI(t)}{dt} &= \beta V(t)S(t)I(t) - \mu I(t), \\
\frac{dT(t)}{dt} &= \Lambda_c - kI(t)T(t)V(t) - \mu_c T(t), \\
\frac{dT^*(t)}{dt} &= kI(t)T(t)V(t) - (\mu_c + \delta_c)T^*(t), \\
\frac{dV(t)}{dt} &= pT^*(t) - cV(t)
\end{aligned} \tag{2.15}$$

The rates of infection k and β are taken to be linear functions of the disease prevalence $I(t)$ and the viral load $V(t)$.

They calculated two threshold quantities, R_h and R_v corresponding to the between host and within host dynamics, respectively and concluded that the magnitudes of these reproduction numbers can determine the prevalence of an infection if considered jointly.

Feng et.al [51] used the linear form of the coupling function to couple the two models. According to work done by Alexis et.al [3], linearly coupling the two models may lead to overestimating the transmission of the disease.

Van *et.al* [31] developed a multiscale model coupling a within host model considering the dynamics of virions and a between host model of EVD. They used the model in exploring Ebola vaccination strategies. Their within host model is

$$\frac{dV(t)}{dt} = rvV(t)\Big(1-\frac{V(t)}{K_v}\Big)\Big(\frac{V(t)}{V(t)+I_N}\Big)\Big(1-\frac{A_b(t)}{K_{Ab}}\Big) \tag{2.16}$$

where $A_b(t)$ is the number of antibodies and $V(t)$, the viral load. The virus replicates in a logistic manner. The replication rate is rv and the carrying capacity of the host is K_v. I_N and K_{Ab} denotes the lag phase threshold and the strength of the immune system respectively. For the between host model, they used the survey data from Europeans' contact patterns [28] to generate the network model. This model reflected the number of contacts, the patterns in which people mix in different age groups and a specific age structure of a population. They chose the city of Freetown in Sierra Leon and used its age distribution as a reference. They then formed a multiscale model by embedding the within host model into the network model they had developed. Some of their results were

(i) In the absence of any intervention, the case fatality rate is 90.93%.

(ii) Interventions can reduce case fatality rate.

(iii) Vaccination can reduce the severity of EVD in people who are newly infected after the program of vaccination.

This study however assumed that the contact pattern of people in Sierra Leone is the same to that of European countries. This may not be true since Sierra Leone is a very poor country and most European countries are highly developed hence there are differences in social and economic status of the people leading to different mixing patterns.

Alexis and Hernandez [2] presented an improved multiscale model of the model by Alexis *et.al* [3]. Their within host model considers the antibody responses of a recovering host from Ebola infection. The model is given below

$$\begin{aligned}\frac{dV(t)}{dt} &= pV(t)\Big(1-\frac{V(t)}{K_v}\Big)\Big(\frac{V(t)}{V(t)+I_N}\Big)\Big(1-\frac{A(t)}{K_A}\Big), V(0)\geq 0,\\ \frac{dA(t)}{dt} &= \delta_A A, A(0)\geq 0. \end{aligned} \tag{2.17}$$

where $A(t)$, $V(t)$, K_v and I_N are as defined in (2.16) while p is the rate of reproduction of the virions.

Their multiscale model is

$$\begin{aligned}\frac{dS(t)}{dt} &= (N_S-\delta_S S(t))-\beta(V)S(t)I(t),\\ \frac{dI(t)}{dt} &= \beta(V)S(t)I(t)-(\delta_I+\gamma)I(t),\\ \frac{dR(t)}{dt} &= \gamma I(t)-\delta_R R(t)\end{aligned} \tag{2.18}$$

From the analysis, the equilibrium points are stable. They considered a saturated form of the coupling function in the simulations and concluded that the time window for effective antibody response determines the time window before an outbreak occurs.

The models in [31] and [2] have considered only the viral dynamics and antibodies leaving the uninfected target cells and infected cells which are very important in EVD dynamics.

In this study, the gaps identified in the literature review have been addressed by developing and analysing a multiscale model coupling a within host model and a between host model via the viral load. The within host model has considered the uninfected cells, infected cells and the virions. It has a saturated incidence rate and the effect of treatment has also been investigated. The between host SEIR model has considered the rate and efficacy of vaccination.

CHAPTER THREE

WITHIN HOST EBOLA MODEL

3.1 Introduction

In this chapter, we have formulated a within host model of EVD incorporating a logistic growth of the target cells, a saturated incidence rate and the effect of treatment. Treatment here encompasses supportive care and the Ebola treatment drugs undergoing clinical trials. We have analysed the local and global stability of the equilibrium points as well as perform numerical simulations to investigate the effect of efficacy of treatment.

3.2 Model Formulation

The dynamics of EVD within a given host is represented mathematically by a nonlinear model consisting of three compartments namely; uninfected cells $X(t)$, infected cells $Y(t)$ and virions $L(t)$. The uninfected cells grow logistically at the rate m. α is the mortality rate of the uninfected cells and Q is the carrying capacity. The uninfected cells interact with the virions $L(t)$ at a constant infectivity rate β. This interaction produces infected cells $Y(t)$ which in turn produce infectious virions $L(t)$ at the rate c and ρ $(0 \leq \rho \leq 1)$ measures the efficacy of treatment.

The infected cells die at the rate η and k determines the saturation level when the virion population is large.

The virions die at the rate γ.

These dynamics are illustrated by the diagram below

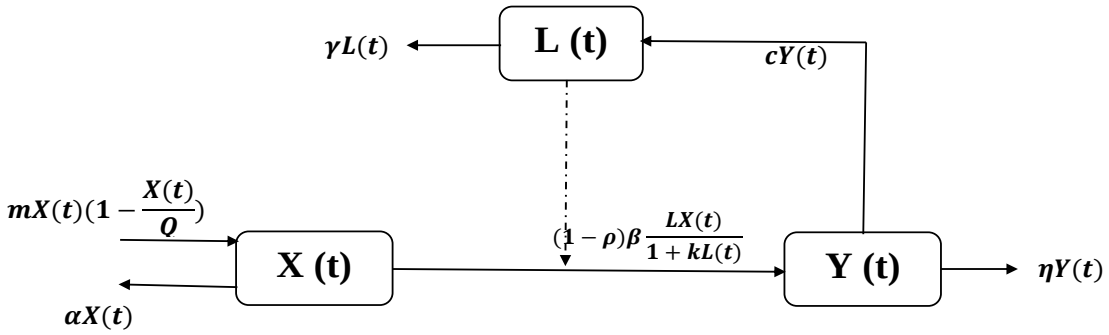

Figure 3.1: Within host Model Flow Chart

The flow diagram above leads us to the system of nonlinear system 3.1

$$\begin{aligned}
\frac{dX(t)}{dt} &= mX(t)\Big(1-\frac{X(t)}{Q}\Big) - (1-\rho)\beta\frac{L(t)X(t)}{1+kL(t)} - \alpha X(t),\\
\frac{dY(t)}{dt} &= (1-\rho)\beta\frac{L(t)X(t)}{1+kL(t)} - \eta Y(t),\\
\frac{dL}{dt} &= cY(t) - \gamma L(t) \qquad (3.1)
\end{aligned}$$

With the conditions $X(0) = X_0$, $Y(0) = Y_0$, $L(0) = L_0$ at $t = 0$.

Model (3.1) is studied in the closed set $\Pi = (X(t), Y(t), L(t)) \in \mathbb{R}^3_+$

Table 3.1 summarizes the variables and parameters that have been used in Model (3.1).

Table 3.1: Description of Parameters and Variables

Variable or Parameter	Description
$X(t)$	The number of uninfected cells which are susceptible to infection.
$Y(t)$	The number of cells which have been infected with Ebola virus and they produce virions which cause infection.
$L(t)$	The number of Ebola virions at any time t.
m	Rate of growth of the uninfected cells.
Q	The carrying capacity of the host
ρ	The efficacy of treatment of EVD.
β	The transmission rate of the virus.
k	The saturation factor.
α	The rate of mortality of the uninfected cells.
η	The mortality rate of infected cells.
c	The production rate of new virions.
γ	Mortality rate of free virions.

3.3 Positivity and Boundedness of solutions

We use the lemma below to study the positivity and boundedness of solutions to equations of Model (3.1).

Lemma 3.3.1. *Let $t_0 > 0$. If $X_0 > 0, Y_0 > 0$ and $L_0 > 0$, then $X(t), Y(t)$ and $L(t)$ will each remain nonnegative and bounded in $\mathbb{R}^3_+$ for all $t \in [0, t_0]$.*

Proof. The first and second equations of model (3.1) represents the population of cells and the last one represents population of virions. These are always positive. Therefore ,they are bounded below.

For the first equation, we have

$$\begin{aligned} \frac{dX(t)}{dt} &= mX(t)\Big(1 - \frac{X(t)}{Q}\Big) - (1-\rho)\beta\frac{L(t)X(t)}{1+kL(t)} - \alpha X(t), \\ &> -(1-\rho)\beta\frac{L(t)X(t)}{1+kL(t)} - \alpha X(t) \end{aligned} \tag{3.2}$$

Solving for $X(t)$ yields $X(t) > X_0 e^{-\alpha t - \beta \int \frac{L(t)}{1+kL(t)} dt} > 0$.

Similarly, the other equations yield $Y(t) > Y_0 e^{-\eta t} > 0$ and $L(t) > L_0 e^{-\gamma t} > 0$ respectively.

In all these three solutions, X_0, Y_0 and L_0 are constants of integration. Therefore, for all $t \in [0, t_0]$, $X(t), Y(t)$ and $L(t)$ will be positive and remain in $\mathbb{R}^3_+$.

Next, we show that all the three equations are ultimately bounded for $t \geq 0$.

For the first equation, the viral infection reduces the population of the target cells so at the onset of infection , the population of uninfected cells must be greater than or equal to the total cell population at $t > 0$. The second and third equations reduce to zero at the Infection Free Equilibrium (IFE).

This leaves us with first equation and since the target cells grow logistically, the number of cells is given by

$$X(t) = \frac{QX_0}{X_0 + (Q - X_0))e^{-mt}} \tag{3.3}$$

For initial population values below the carrying capacity Q, the population of cells grows to Q as time increases as shown below;

$$\lim_{t\to\infty} X(t) = \lim_{t\to\infty} \frac{QX_0}{X_0 + (Q - X_0)e^{-mt}} \tag{3.4}$$

$$= Q \tag{3.5}$$

Thus, the Model (3.1) is bounded above by Q and bounded below by 0.

Since model (3.1) is positive and bounded, it is well posed in the considered region Π. □

3.4 The Infection Free Equilibrium

Infection Free Equilibrium, (IFE) of a model is its steady state solution at which no infection (or disease) is present. It is obtained by setting the right hand side of model (3.1) to zero and solving for the state variables with $Y(t) = L(t) = 0$. This gives $X(t) = Q - \frac{\alpha Q}{m}$. Therefore the IFE is $[X^0, Y^0, L^0]$=$[Q - \frac{\alpha Q}{m}, 0, 0]$.

3.4.1 Evaluation of the Basic Reproduction number, (R_0^w)

The basic reproduction number is the expected number of infections generated by a single infectious cell introduced in a population of uninfected cells which are susceptible to infection. R_0^w is obtained using the method of next generation matrix [42].

The infection compartments in this model are $Y(t)$ and $L(t)$. The rate of increase in infection and the rate of progression of infection in the i^{th} infection compartment are denoted by $\mathcal{F}_i$ and $\mathcal{V}_i$ respectively. Thus for model (3.1),

$$\begin{aligned} \mathcal{F} &= \begin{pmatrix} (1-\rho)\beta\frac{L(t)X(t)}{1+kL(t)} \\ 0 \end{pmatrix} \\ \mathcal{V} &= \begin{pmatrix} \eta Y(t) \\ \gamma L - cY \end{pmatrix}. \end{aligned} \tag{3.6}$$

Differentiating $\mathcal{F}_i$ and $\mathcal{V}_i$ with respect to $Y(t)$ and $L(t)$ and evaluating them at Infection Free Equilibrium E_0 gives

$$\begin{aligned} F &= \left(\frac{\partial \mathcal{F}_i(E_0)}{\partial x_j}\right) \\ V &= \left(\frac{\partial \mathcal{V}_i(E_0)}{\partial x_j}\right) \end{aligned} \tag{3.7}$$

Hence, the matrix F and matrix V are respectively given by

$$F = \begin{pmatrix} 0 & (1-\rho)\beta Q(1-\frac{\alpha}{m}) \\ 0 & 0 \end{pmatrix}$$

and

$$V = \begin{pmatrix} \eta & 0 \\ -c & \gamma \end{pmatrix} \tag{3.8}$$

so that

$$V^{-1} = \begin{pmatrix} \frac{1}{\eta} & 0 \\ \frac{c}{\eta\gamma} & \frac{1}{\gamma} \end{pmatrix} \tag{3.9}$$

Therefore,

$$FV^{-1} = \begin{pmatrix} \frac{(1-\rho)\beta Q(1-\frac{\alpha}{m})c}{\eta\gamma} & \frac{(1-\rho)\beta Q(1-\frac{\alpha}{m})}{\gamma} \\ 0 & 0 \end{pmatrix} \tag{3.10}$$

The reproduction number, R_0^w is given by the spectral radius of matrix FV^{-1}. Hence,

$$R_0^w = \frac{(1-\rho)\beta c Q(1-\frac{\alpha}{m})}{\eta\gamma} \tag{3.11}$$

3.4.2 Local Stability Analysis of the Infection Free Equilibrium

This is investigated using the theorem below.

Theorem 3.4.1. *If $R_0^w < 1$, then $E_0 = [Q - \frac{\alpha Q}{m}, 0, 0]$ is locally asymptotically stable.*

Proof. The Jacobian of model (3.1) is given by

$$J = \begin{pmatrix} m - \alpha - \frac{2mX(t)}{Q} - (1-\rho)\frac{\beta L(t)}{1+kL(t)} & 0 & -\frac{(1-\rho)\beta X(t)}{(1+kL(t))^2} \\ (1-\rho)\frac{\beta L(t)}{1+kL(t)} & -\eta & \frac{(1-\rho)\beta X(t)}{(1+kL(t))^2} \\ 0 & c & -\gamma \end{pmatrix} \tag{3.12}$$

At Infection Free Equilibrium (IFE), $Y(t) = L(t) = 0$ and $X(t) = Q - \frac{\alpha Q}{m}$.

Evaluating matrix (3.12) at IFE, we have

$$J(E_0) = \begin{pmatrix} \alpha - m & 0 & -(1-\rho)\beta(Q - \frac{\alpha Q}{m}) \\ 0 & -\eta & (1-\rho)\beta(Q - \frac{\alpha Q}{m}) \\ 0 & c & -\gamma \end{pmatrix} \tag{3.13}$$

One of the eigenvalues of the matrix (3.13) is

$$\lambda = \alpha - m \tag{3.14}$$

which is negative since $m > \alpha$. (The population of target cells must always be greater than zero. For this to be possible, birth rate must be greater than death rate.)

To determine the nature of the other eigenvalues, the reduced matrix below is considered.

$$J_R = \begin{pmatrix} -\eta & \frac{\eta\gamma}{c} R_0^w \\ c & -\gamma \end{pmatrix} \tag{3.15}$$

The trace of the matrix (3.15) is given by $-(\eta + \gamma) < 0$ and the determinant is given by $\eta\gamma(1 - R_0^w)$. This determinant is positive when $\eta\gamma(1 - R_0^w) > 0$, that is $R_0^w < 1$.

The Routh Hurwitz criterion guaranteeing the existence of eigenvalues with negative real part has been met.

Therefore the IFE is locally asymptotically stable whenever $R_0^w < 1$. Otherwise, it is unstable.

Epidemiologically this means that if a single virion is introduced into a fully susceptible population of uninfected cells, the infection would die out whenever $R_0^w < 1$. Otherwise the infection would spread to other cells. □

3.5 Global Stability Analysis of the Infection Free Equilibrium

This analysis is done using the theorem by Castillo *et. al* [7] as described below.

Rewrite model (3.1) in the form;

$$\begin{aligned} \frac{dM(t)}{dt} &= F(M(t), Z(t)) \\ \frac{dZ(t)}{dt} &= G(M(t), Z(t)), \quad G(M(t), 0) = 0 \end{aligned} \tag{3.16}$$

where $M(t) = X(t)$ denotes the total number of uninfected cells while $Z(t) = (Y(t), L(t))$, denotes the number of infected cells and the number of free virions respectively. The IFE is now given by

$$E_0 = (M_0, 0) \quad \text{where} \quad M_0 = Q - \frac{\alpha Q}{m}$$

For the IFE to be globally asymptotically stable, conditions H_1 and H_2 below must be met

.

H_1: $\frac{dM(t)}{dt} = F(M(t), 0)$, E_0 is globally asymptotically stable.

H_2: $G(M(t), Z(t)) = PZ(t) - \hat{G}(M(t), Z(t))$

where $\hat{G}(M(t), Z(t)) \geq 0$ and $P = D_Z G(E_0, 0)$ is a metzler matrix.

Theorem 3.5.1. *$E_0 = (M_0, 0)$ is a globally asymptotically stable equilibrium of model (3.1) provided $R_0^w < 1$ and the assumptions H_1 and H_2 are met.*

Proof. We have

$$\begin{aligned}
\frac{dM(t)}{dt} = F(M(t), Z(t)) &= mX(1 - \frac{X}{Q}) - (1-\rho)\beta\frac{L(t)X(t)}{1+kL(t)} - \alpha X(t) \\
\text{At the IFE, Z(t)=0 so} \quad F(M(t), 0) &= mX(1 - \frac{X}{Q}) - \alpha X(t) \\
\frac{dZ(t)}{dt} &= G(M(t), Z(t)) = \begin{pmatrix} (1-\rho)\beta\frac{L(t)X(t)}{1+kL(t)} - \eta Y(t) \\ cY(t) - \gamma L(t) \end{pmatrix} \\
\text{and } G(M(t), 0) &= 0
\end{aligned}$$

Therefore

$$\begin{aligned}
\frac{dM(t)}{dt} = F(M(t), 0) &= mX(1 - \frac{X}{Q}) - \alpha X(t) \\
P = D_Z G(M_0, 0) &= \begin{pmatrix} -\eta & (1-\rho)\beta Q(1 - \frac{\alpha}{m}) \\ c & -\gamma \end{pmatrix} \\
PZ(t) &= \begin{pmatrix} -\eta & (1-\rho)\beta Q(1 - \frac{\alpha}{m}) \\ c & -\gamma \end{pmatrix} \begin{pmatrix} Y(t) \\ L(t) \end{pmatrix} \\
&= \begin{pmatrix} (1-\rho)\beta M_0 L(t) - \eta Y(t) \\ cY(t) - \gamma L(t) \end{pmatrix} \qquad (3.17)
\end{aligned}$$

and

$$\hat{G}(M(t), Z(t)) = \begin{pmatrix} \hat{G}_1(M(t), Z(t)) \\ \hat{G}_2(M(t), Z(t)) \end{pmatrix} = \begin{pmatrix} 0 \\ 0 \end{pmatrix} \qquad (3.18)$$

$$\text{since} \quad M_0 = \frac{X(t_0)}{1 + kL(t_0)} \qquad (3.19)$$

Equation (3.18) shows that $\hat{G}(M(t), Z(t)) \geq 0$. Conditions H_1 and H_2 have been satisfied and thus E_0 is globally asymptotically stable for $R_0^w < 1$. This means that if you give the system a large pertubation, it will return to the IFE. □

3.6 The endemic equilibrium point

The endemic equilibrium point is an equilibrium in which the infection is present in the population of the cells. Ebola virus infection within the host is endemic if $X^*(t) > 0, Y^*(t) > 0$ and $L^*(t) > 0$ for all $t > 0$.

3.6.1 Existence of the endemic equilibrium point

This is shown using the lemma below.

Lemma 3.6.1. *The Ebola virus infection exists and is persistent in the population whenever* $R_0^w > 1$.

Proof. At endemic equilibrium, the equation of free virions in model (3.1) gives $L^*(t) = \frac{cY^*(t)}{\gamma}$ and the limiting value of $X(t)$ is $Q - \frac{\alpha Q}{m}$.
Substituting these two expressions in the equation of infected cells in model (3.1), we get

$$\beta Q(1-\rho)(1-\frac{\alpha}{m})\frac{cY^*(t)}{\gamma + kcY^*(t)} - \eta Y^*(t) = 0. \tag{3.20}$$

Equivalently, Equation (3.20) can be written as

$$\frac{\eta R_0^w}{\gamma + kcY^*(t)} - \eta = 0 \tag{3.21}$$

giving

$$Y^*(t) = \frac{\gamma}{kc}[R_0^w - 1] \tag{3.22}$$

on further simplification.
Equation (3.22) shows that $Y^*(t) > 0$ if and only if $R_0^w > 1$. This means that the EE point exists whenever $R_0^w > 1$ □

We therefore get the endemic equilibrium point as shown below.
Using Equation (3.22), $L^*(t)$ can now be written as

$$L^*(t) = \frac{1}{k}[R_0^w - 1] \tag{3.23}$$

Making $X(t)$ the subject in the equation of the uninfected cells in model (3.1) and substituting the value of $L^*(t)$ from Equation (3.23) gives
$X^*(t) = (1-\rho)\frac{\beta Q}{kmR_0^w}(1-R_0^w) + (1-\frac{\alpha}{m})Q$. Thus we have the EE point $\Big[X^*(t), Y^*(t), L^*(t)\Big]$ given by

$$\Big[\Big(1-\rho\Big)\frac{\beta Q}{kmR_0^w}\Big(1-R_0^w\Big) + \Big(1-\frac{\alpha}{m}\Big)Q, \frac{\gamma}{kc}\Big(R_0^w - 1\Big), \frac{1}{k}\Big(R_0^w - 1\Big)\Big] \tag{3.24}$$

3.6.2 Stability analysis of the endemic equilibrium point

We use the Center Manifold Theorem [23] as illustrated below.

Theorem 3.6.1. *Consider the following general system of ODEs.* $\frac{dx}{dt} = f(x, \phi), f : \mathbb{R}^n \times \mathbb{R} \to \mathbb{R}^n$ *and* $f \in C^2(\mathbb{R}^n \times \mathbb{R})$

Let the origin be an equilibrium point of this systemnfor all values of ϕ *where* ϕ *is a parameter. Let*

1 . $F = D_x f(0, 0)$

2 . *Zero is an eigenvalue of* F *and each of the remaining eigenvalues of* F *has a real part that is negative.*

3 . *Matrix* F *has a right eigenvector* $w = (w_1, w_2, w_3)^T$ *and a left eigenvector* $v = (v_1, v_2, v_3)^T$ *each of which corresponds to the zero eigenvalue*

Let

$$s^\star = \sum_{k,i,j=1}^{n} v_k w_i w_j \frac{\partial^2 f_k}{\partial x_i \partial x_j}(0, 0),$$

$$r^\star = \sum_{k,i=1}^{n} v_k w_i \frac{\partial^2 f_k}{\partial x_i \partial \beta^\star}(0, 0)$$

The signs of $s^\star$ *and* $r^\star$ *determines the dynamics of the given system around the equilibrium point at the origin. Specifically;*

(i) $s^\star > 0; r^\star > 0$ *when* $\beta^\star < 0$*, with* $|\beta^\star < 0| \ll 1$*, (0,0) is locally asymptotically stable and there exist a positive unstable equilibrium; when* $0 < \beta^\star \ll 1$*, (0,0) is unstable and there exists a negative and locally asymptotically stable equilibrium.*

(ii) $s^\star < 0; r^\star < 0$*, when* $\beta^\star < 0$ *with* $|\beta^\star| \ll 1$ *(0,0) is unstable; when* $0 < \beta^\star \ll 1$*, (0,0) is locally asymptotically stable, and there exists a positive unstable equilibrium.*

(iii) $s^\star > 0; r^\star < 0$*, when* $\beta^\star < 0$ *with* $|\beta^\star| \ll 1$*, (0,0) is unstable and there exists a negative and locally asymptotically stable equilibrium, when* $0 < \beta^\star \ll 1$*, (0,0) is stable and there exists a positive unstable equilibrium.*

(iv) $s^\star < 0; r^\star > 0$, *when* $\beta^\star < 0$ *changes from negative to positive, (0,0) changes its stability from stable to unstable. Correspondingly, a negative unstable equilibrium becomes positive and locally asymptotically stable.*

Applying theorem (3.6.1),we proceed as follows;

Let $X(t) = u_1, Y(t) = u_2$ and $L(t) = u_3$.

The model 3.1 can be written in the form

$$\frac{dU}{dt} = F(u)$$

where

$$U = (u_1, u_2, u_3)$$

$$F = (f_1, f_2, f_3)$$

so that

$$\begin{aligned} \frac{du_1}{dt} &= mu_1(1 - \frac{u_1}{Q}) - (1-\rho)\beta\frac{u_3u_1}{1+u_3} - \alpha u_1, \\ \frac{du_2}{dt} &= (1-\rho)\beta\frac{u_3u_1}{1+ku_3} - \eta u_2, \\ \frac{du_3}{dt} &= cu_2 - \gamma u_3 \end{aligned} \tag{3.25}$$

The Jacobian matrix of model (3.25) at the IFE is given by matrix (3.13)

To analyze the dynamics of model (3.25), we compute the right and left eigenvectors of matrix (3.13). Thus

$$\begin{pmatrix} \alpha - m & 0 & -(1-\rho)\beta(Q - \frac{\alpha Q}{m}) \\ 0 & -\eta & (1-\rho)\beta(Q - \frac{\alpha Q}{m}) \\ 0 & c & -\gamma \end{pmatrix} \begin{pmatrix} w_1 \\ w_2 \\ w_3 \end{pmatrix} = \begin{pmatrix} 0 \\ 0 \\ 0 \end{pmatrix} \tag{3.26}$$

This gives the entries of the right eigenvector as $w_1 = \frac{w_2\eta}{\alpha - m}$, $w_2 = w_2 > 0$ and $w_3 = \frac{cw_2}{\gamma}$

To obtain the left eigenvector, evaluate

$$\begin{pmatrix} v_1 & v_2 & v_3 \end{pmatrix} \begin{pmatrix} \alpha - m & 0 & -(1-\rho)\beta(Q - \frac{\alpha Q}{m}) \\ 0 & -\eta & (1-\rho)\beta(Q - \frac{\alpha Q}{m}) \\ 0 & c & -\gamma \end{pmatrix} = \begin{pmatrix} 0 & 0 & 0 \end{pmatrix} \tag{3.27}$$

This gives the entries of the left eigenvector as $v_1 = 0$, $v_2 = \frac{\gamma v_3}{(1-\rho)\beta Q(1-\frac{\alpha}{m})}$ and $v_3 = v_3 > 0$

Then calculate $s^\star$ as follows;

For the transformed model (3.25), the associated nonzero partial differentials of f evaluated at the IFE, (E_0) are each 0 except

$$\frac{\partial^2 f_2}{\partial x_1 \partial x_2}(0,0) \quad = \quad (1-\rho)\beta$$

Therefore $s^\star = (1-\rho)\beta\frac{v_2{\omega_2}^2\eta}{\gamma(\alpha-m)} < 0$ [Since $m > \alpha$]

Consider the case when $R_0^w = 1$ and choose $\beta = \beta^*$ as a bifurcation parameter. Solving for β^* from $R_0^w = 1$ gives

$$\beta^* = \frac{\eta\gamma}{(1-\rho)cQ(1-\frac{\alpha}{m})} \tag{3.28}$$

Similarly, in getting $r^\star$, the associated nonzero partial differentials of f evaluated at the IFE, (E_0) are each 0 except

$$\frac{\partial^2 f_2}{\partial x_1 \partial \beta}(0,0) \quad = \quad (1-\rho)$$

and

$$\frac{\partial^2 f_2}{\partial x_3 \partial \beta}(0,0) \quad = \quad (1-\rho)Q(1-\frac{\alpha}{m})$$

Therefore

$$r^\star = v_2 w_1 \frac{\partial^2 f_2}{\partial x_1 \partial \beta}(0,0) + v_2 w_3 \frac{\partial^2 f_2}{\partial x_3 \partial \beta}(0,0)$$

$$= (1-\rho)v_2\omega_2\Big[\frac{\eta}{\alpha-m} + \frac{cQ}{\gamma}(1-\frac{\alpha}{m})\Big] > 0$$

Since $s^\star < 0$ and $r^\star > 0$, theorem (3.6.1) holds. Thus, Model (3.25) has a unique endemic equilibrium which is locally asymptotically stable whenever $R_0^w > 1$ and unstable when $R_0^w < 1$.

3.7 Numerical Simulations and Discussions

MATLAB Software is used here in simulating model (3.1) so as to illustrate the long term behavior of the state variables and to show the impact of treatment.

The set of parameters used are presented in Table 3.2 while the results are depicted by Figures 3.2 to 3.5.

Table 3.2: Values of parameters

Parameter	Description	units	Value	source
m	Growth rate of uninfected cells	$ml^{-1}day^{-1}$	0.1-10	[39]
Q	Carrying capacity of the host	mm^{-3}	1500	[36]
ρ	Efficacy of treatment		$(0 \leq \rho \leq 1)$	varies
β	Transmission rate	day^{-1}	0.0027	[39]
k	Saturation factor	day^{-1}	0.001	[36]
α	Mortality rate of uninfected cells	day^{-1}	0.02	[39]
η	Mortality rate of Infected cells	day^{-1}	0.24	[39]
c	Rate of producing new virions	day^{-1}	2.4	[36]
γ	Mortality rate of free virions	day^{-1}	2	[36]

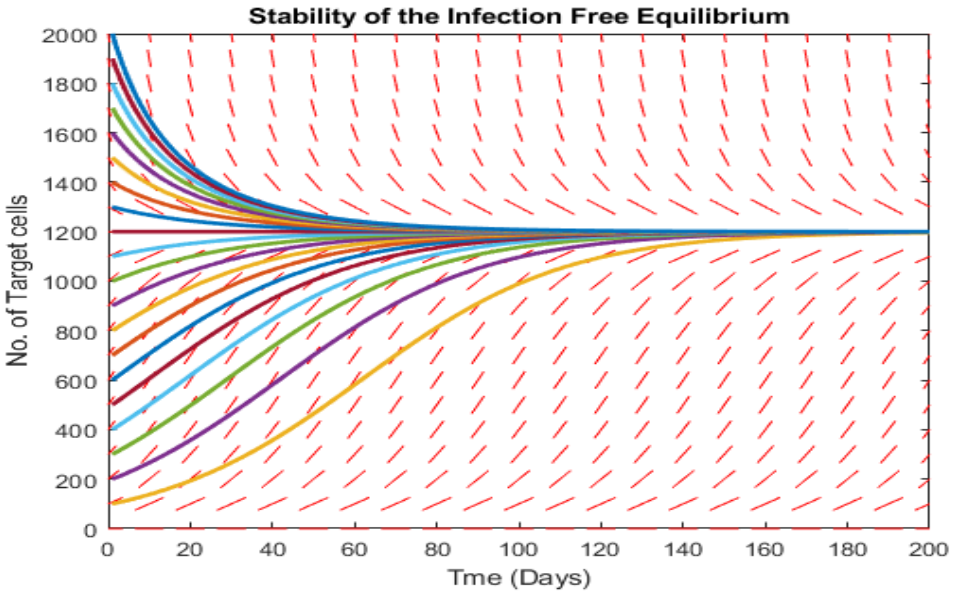

Figure 3.2: Stability of IFE

From Figure 3.2, we observe that in the absence of infection and taking $m = 0.1, \alpha = 0.02$ and $Q = 1500$, the model (3.1) has an IFE given by $I_0[1200, 0, 0]$ and it is globally asymptotical stable. This is consistent with our theoretical analysis done in this study.

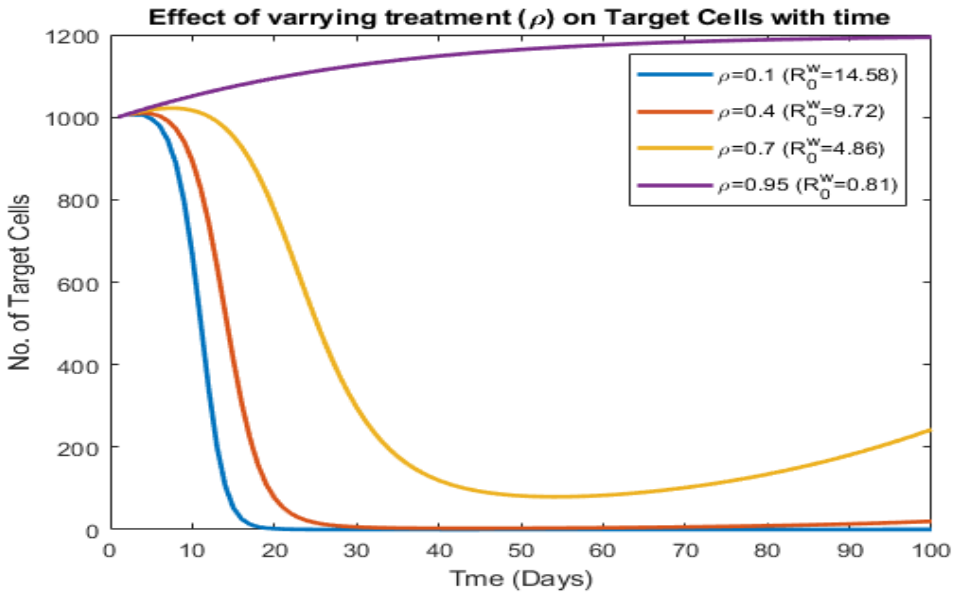

Figure 3.3: Effect of varying ρ on Evolution of Target cells

Figure 3.3 above shows changes in the number of uninfected cells for different efficacies of treatment as time changes. It is expected that the number of target cells reduce with time since some of the cells get infected whenever $R_0^w > 1$. When treatment efficacy is lower (e.g $\rho = 0.1$), the target cells are depleted faster as opposed to when the treatment efficacy is slightly increased (e.g $\rho = 0.4$). When $\rho = 0.7$, the target cells reduce at a lower rate and they don't get depleted. However, when $\rho = 0.95$, there are no new infections since $R_0^w = 0.81 < 1$. This makes the target cells to grow and reach the Infection free equilibrium.

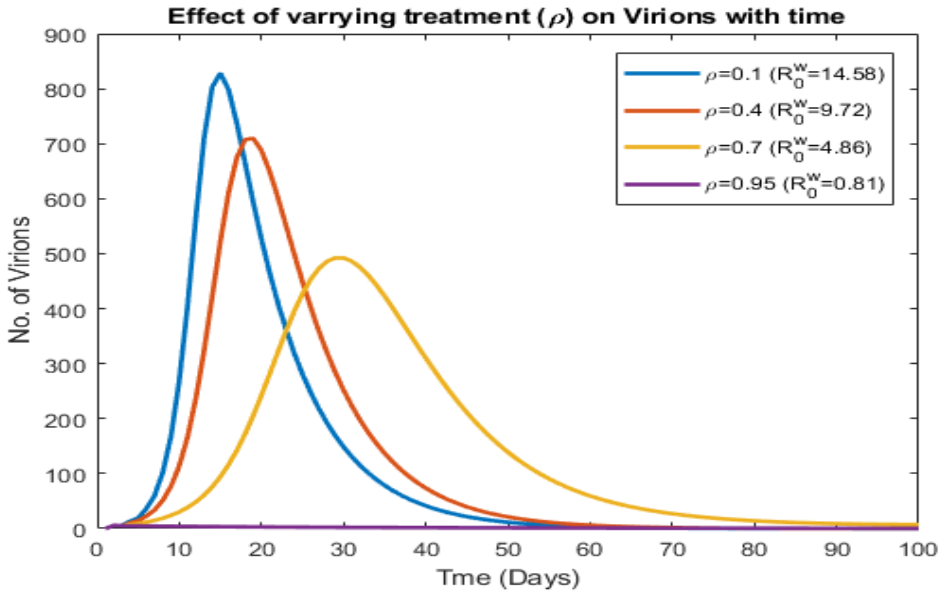

Figure 3.4: Effect of varying ρ on Evolution of Virions

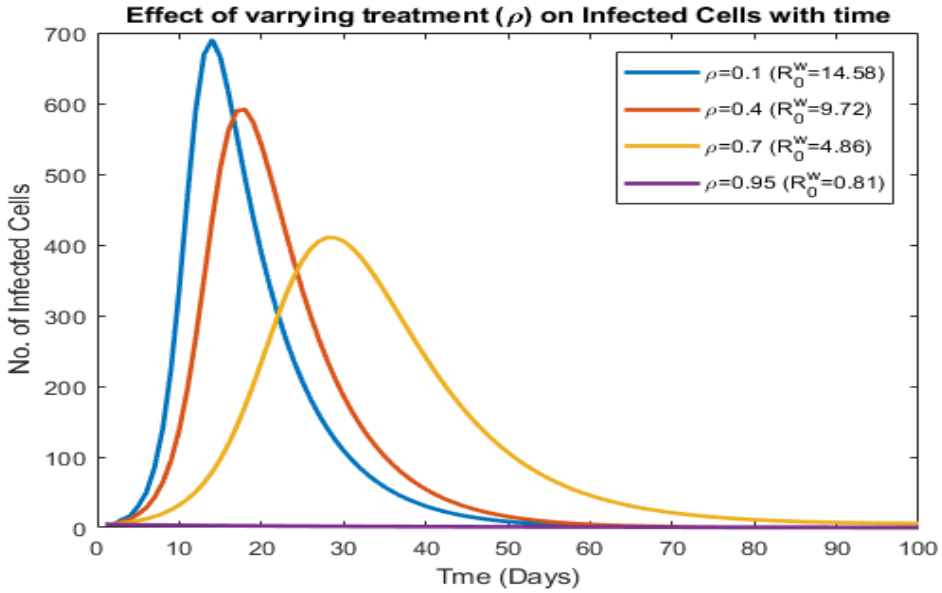

Figure 3.5: Effect of varying ρ on Evolution of Infected cells

From Figure 3.4, it can be observed that the number of free virions increase sharply within the first few days because of poor immune response resulting from a low efficacy of treatment, reaching the peak of about 850 virions per mililitre in day 14 (depicted by the blue line) when $\rho = 0.1$. Consequently, the number of infected cells increase in a similar manner since they are generated by the free virions, as shown in Figure 3.5.

However, when the efficacy of treatment is higher (e.g $\rho = 0.7$) thereby lowering R_0^W, the number of free virions and the infected cells is kept low.

Ebola virus has been noted to be undetectable by the body's immune system within the first few days of invasion. This is because Ebola virus attacks the dendritic cells which are responsible for activating the immune response against the virus. This makes the virus to begin replicating immediately and rapidly [21] in the first few days and especially in the case of low and medium efficacy of treatment. However, after some days, the sharp increase noted begins to decline. This may be attributed to the fact that the invading pathogen has been identified and an appropriate immune response mounted with the help of treatment strategies employed. When treatment has a very high efficacy ($\rho = 0.95$), $R_0^W < 1$ meaning there are no new infections realised and hence no new virions produced. This is clearly depicted in Figure 3.4 and Figure 3.5.

CHAPTER FOUR

BETWEEN HOST EBOLA MODEL

4.1 Introduction

A between host model of Ebola virus Disease is developed and analysed in this chapter. We begin by describing and formulating the model then test for positivity and boundedness of solutions, perform stability analyses for the equilibrium points and do simulations using MATLAB software.

4.2 Assumptions in the model

(i) The population is homogeneous; therefore each individual has the same probability of entering into a compartment.

(ii) Recovered individuals acquire temporary immunity

4.3 Description and Formulation of the model

The between host dynamics of EVD is described by a nonlinear model having four classes of individuals namely; the susceptible, the exposed, the infected and the recovered. These are respectively denoted by $S(t)$, $E(t)$, $I(t)$ and $R(t)$. All the classes have natural death rate μ.

Susceptible individuals become infected at the rate λ through interactions with the infected individuals while the vaccinated ones are infected at a reduced rate λv through the same interaction. Those who have been exposed to EVD become symptomatic and proceed to the infected class at the rate σ. The disease induced death rate for the infected individuals is ψ and they recover at the rate ω.

These dynamics are illustrated by the schematic diagram below

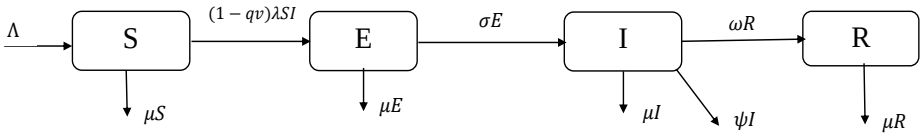

Figure 4.1: Flow Diagram of Model (4.1)

The schematic diagram leads us to the following system of ODEs.

$$\begin{aligned}
\frac{dS(t)}{dt} &= \Lambda - (1-qv)\lambda S(t)I(t) - \mu S(t), \\
\frac{dE(t)}{dt} &= (1-qv)\lambda S(t)I(t) - \sigma E(t) - \mu E(t), \\
\frac{dI(t)}{dt} &= \sigma E(t) - (\omega + \psi + \mu)I(t), \\
\frac{dR(t)}{dt} &= \omega I(t) - \mu R(t)
\end{aligned} \tag{4.1}$$

Table 4.1 explains the descriptions of the parameters and variables of the model.

Table 4.1: Parameters and Variables of Model (4.1)

Symbol	Description of parameter/ variable.
$S(t)$	The number of susceptible individuals.
$E(t)$	The number of infected individuals who are not showing symptoms.
$I(t)$	The number of infected individuals who have symptoms of EVD and are infectious.
$R(t)$	The number of recovered individuals.
Λ	The rate of recruitment of the susceptibles
λ	The rate of infection.
μ	The natural death rate.
q	The efficacy of vaccine.
v	The rate of vaccination.
σ	The rate of development of symptoms.
ψ	Mortality rate induced by EVD.
ω	Rate of Recovery from EVD.

In this model, $N(t) = S(t) + E(t) + I(t) + R(t)$ gives the total human population and the initial population is N_0.

4.4 Positivity and Boundedness of Solutions

With reference to Model (4.1), we show that the solutions are bounded.

$$\begin{aligned} \frac{dN(t)}{dt} &= \frac{d}{dt}\Big(S(t)+E(t)+I(t)+R(t)\Big), \\ &= \Lambda-\mu N(t)-\psi I(t), \\ \frac{dN(t)}{dt} &< \Lambda-\mu N(t) \end{aligned} \tag{4.2}$$

(by Comparison Theorem [19]).

Separating the variables and integrating gives

$$\begin{aligned} \int \frac{dN(t)}{\Lambda-\mu N(t)} &< \int dt, \\ N(t) &< \frac{\Lambda}{\mu}-ke^{-\mu t} \end{aligned} \tag{4.3}$$

We therefore have

$$N(t) < \frac{\Lambda}{\mu}\Big(1-e^{-\mu t}\Big)+N_0e^{-\mu t} \tag{4.4}$$

As $t \longrightarrow \infty$, $N(t) \longrightarrow \frac{\Lambda}{\mu}$. This shows that $N(t)$ is bounded; $0 < N(t) < \frac{\Lambda}{\mu}$

and so this model is feasible in set Ω, where

$\Omega = \Big\{\Big(S(t),E(t),I(t),R(t)\Big) \in \mathbb{R}^4_+ | 0 < N(t) < \frac{\Lambda}{\mu}\Big\}$

Next, we show that the state variables $S(t), E(t), I(t)$ and $R(t)$ are all nonnegative for all time $t \geq 0$ using the lemma below.

Lemma 4.4.1. *The solutions of equations of the Model (4.1), will remain nonnegative for all $t \geq 0$ in the region Ω.*

Proof. Considering the first equation of the Model, we have;

$$\begin{aligned} \frac{dS(t)}{dt} &= \Lambda - (1-qv)\lambda S(t)I(t) - \mu S(t), \\ &> -\Big((1-qv)\lambda I(t) + \mu\Big)S(t) \end{aligned} \tag{4.5}$$

resulting in $S(t) > S_0 e^{\left[-\int_0^t \left((1-qv)\lambda I(\xi)+\mu\right)\right]d\xi} > 0$.

In a similar manner, the second, third and fourth equations of model (4.1)yields

$E(t) > E_0 e^{[-\int_0^t (\sigma+\mu)d\xi]} > 0$, $I(t) > I_0 e^{[-\int_0^t (\omega+\psi+\mu)d\xi]} > 0$ and $R(t) > R_0 e^{[-\int_0^t (\mu)d\xi]} > 0$ respectively.

Hence all solutions of equations of model (4.1) remain non negative at any time t. □

In this model, those who have recovered do not affect the dynamics of the disease in any way. Consequently, the recovered class is not considered in the analysis.

4.5 The Disease Free Equilibrium

The Disease Free Equilibrium (DFE) point of a model is the equilibrium point where the disease is not present. To get the DFE, equate the right hand side of equations of model (4.1) to zero and solve for $S(t)$ with $E(t)$=$I(t) = 0$. This gives us $S^0 = \frac{\Lambda}{\mu}$. Therefore the DFE is Γ_0=$[\frac{\Lambda}{\mu}, 0, 0]$.

4.6 The Basic Reproduction number

This is the average number of secondary infections produced by an infectious individual introduced in a population of fully susceptible individuals during the entire period of infectivity. From the model (4.1), the transmission and the transition matrices are given by

$$\begin{aligned} F &= \begin{pmatrix} 0 & \frac{(1-qv)\lambda\Lambda}{\mu} \\ 0 & 0 \end{pmatrix} \text{ and} \\ V &= \begin{pmatrix} \sigma+\mu & 0 \\ -\sigma & \omega+\psi+\mu \end{pmatrix} \end{aligned} \tag{4.6}$$

respectively. Hence

$$FV^{-1} = \begin{pmatrix} 0 & \frac{(1-qv)\lambda\Lambda}{\mu} \\ 0 & 0 \end{pmatrix} \begin{pmatrix} \frac{1}{\sigma+\mu} & 0 \\ \frac{\sigma}{(\sigma+\mu)(\omega+\psi+\mu)} & \frac{1}{\omega+\psi+\mu} \end{pmatrix}$$

$$= \begin{pmatrix} \frac{(1-qv)\lambda\Lambda\sigma}{\mu(\sigma+\mu)(\omega+\psi+\mu)} & \frac{(1-qv)\lambda\Lambda\sigma}{\mu(\omega+\psi+\mu)} \\ 0 & 0 \end{pmatrix} \tag{4.7}$$

The reproduction number R_0^B is given by the spectral radius of the matrix (4.7), (See [12]). Therefore,

$$R_0^B = \frac{(1-qv)\lambda\Lambda\sigma}{\mu(\sigma+\mu)(\omega+\psi+\mu)} \tag{4.8}$$

4.7 Stability Analysis of the Disease Free Equilibrium

4.7.1 Local Stability Analysis

The local stability is analysed using the theorem below.

Theorem 4.7.1. *If $R_0^B < 1$, then the DFE, $\Gamma_0 = [\frac{\Lambda}{\mu}, 0, 0]$ is locally asymptotically stable.*

Proof. The Jacobian matrix of model (4.1) is given by

$$J = \begin{pmatrix} -(1-qv)\lambda I(t) - \mu & 0 & -(1-qv)\lambda S(t) \\ (1-qv)\lambda I(t) & -\sigma-\mu & (1-qv)\lambda S(t) \\ 0 & \sigma & -(\omega+\psi+\mu) \end{pmatrix} \tag{4.9}$$

At the DFE, matrix (4.9) becomes

$$J(\Gamma_0) = \begin{pmatrix} -\mu & 0 & \frac{-(1-qv)\lambda\Lambda}{\mu} \\ 0 & -\sigma-\mu & \frac{(1-qv)\lambda\Lambda}{\mu} \\ 0 & \sigma & -(\omega+\psi+\mu) \end{pmatrix} \tag{4.10}$$

One of the eigenvalues of matrix (4.10) is $-\mu$. The nature of the other eigenvalues can be determined using the matrix below.

$$J_R = \begin{pmatrix} -(\sigma+\mu) & \frac{(1-qv)\lambda\Lambda}{\mu} \\ \sigma & -(\omega+\psi+\mu) \end{pmatrix} \tag{4.11}$$

The trace of the matrix (4.11) is given by $-(\sigma+\mu)-(\omega+\psi+\mu)$ which is less than 0. Its determinant is given by

$$\begin{aligned} DetJ_R &= (\sigma+\mu)(\psi+\mu+\omega)-\frac{(1-qv)\lambda\Lambda\sigma}{\mu} \\ &= (\sigma+\mu)(\psi+\mu+\omega)\Big[1-R_0^B\Big] \end{aligned} \tag{4.12}$$

The determinant given by Equation (4.12) is positive whenever $R_0^B < 1$.

These show that matrix (4.11) has met the Routh Hurwitz criterion which guarantee the existence of eigenvalues whose real parts are negative. Hence, the DFE is locally asymptotically stable whenever $R_0^B < 1$. □

4.7.2 Global Stability Analysis of the Disease Free Equilibrium

The theorem by Castillo *et. al* [7] is used in this section to determine if the DFE is globally stable or not.

The model (4.1) is rewritten in the form;

$$\begin{aligned} \frac{dM(t)}{dt} &= F(M(t),Z(t)) \\ \frac{dZ(t)}{dt} &= G(M(t),Z(t)), \quad G(M(t),0)=0 \end{aligned} \tag{4.13}$$

where $M(t)=S(t)$ and $Z(t)=(E(t),I(t))$, with $M(t)\in\mathbb{R}_+$ representing the total number of susceptible individuals and $Z(t)\in\mathbb{R}_+^2$ denoting the number of latently infected individuals and the number of symptomatic infected individuals respectively.

The DFE is then denoted by

$$\Gamma_0=(M_0,0) \quad \text{where} \quad M_0=\frac{\Lambda}{\mu}$$

The technique stipulates that the following conditions H_1 and H_2 must be met to guarantee global asymptotic stability.

H_1: $\frac{dM(t)}{dt}=F(M(t),0)$, Γ_0 is globally asymptotically stable.

H_2: $G(M(t),Z(t))=PZ(t)-\hat{G}(M(t),Z(t))$, $\hat{G}(M(t),Z(t))\geq 0$

for $((M(t),Z(t))\in\Omega$ where $P=D_ZG(\Gamma_0,0)$ is an M matrix and Ω is the region where the model is defined.

Theorem 4.7.2. *The fixed point $\Gamma_0 = (M_0, 0)$ is a globally asymptotically stable equilibrium point of model (4.1) provided $R_0^B < 1$ and the assumptions H_1 and H_2 are satisfied.*

Proof.

$$\begin{aligned}
\frac{dM(t)}{dt} = F(M(t), Z(t)) &= \Lambda - (1-v)\lambda S(t)I(t) - (1-q)v\lambda S(t)I(t) - \mu S(t) \\
F(M(t), 0) &= \Lambda - \mu S(t) \\
\frac{dZ(t)}{dt} &= G(M(t), Z(t)) = \begin{pmatrix} (1-v)\lambda S(t)I(t) + (1-q)v\lambda S(t)I(t) - (\sigma+\mu)E(t) \\ \sigma E(t) - (\omega+\psi+\mu)I(t)) \end{pmatrix} \\
\text{and } G(M(t), 0) &= 0
\end{aligned}$$

Therefore

$$\begin{aligned}
\frac{dM(t)}{dt} = F(M(t), 0) &= \Lambda - \mu S(t) \\
P = D_Z G(M_0, 0) &= \begin{pmatrix} -\sigma - \mu & \frac{(1-qv)\lambda\Lambda}{\mu} \\ \sigma & -(\omega+\psi+\mu) \end{pmatrix} \\
\text{and } \hat{G}(M(t), Z(t)) &= \begin{pmatrix} \hat{G}_1(M(t), Z(t)) \\ \hat{G}_2(M(t), Z(t)) \end{pmatrix} = \begin{pmatrix} 0 \\ 0 \end{pmatrix}
\end{aligned}$$

We see that $\hat{G}(M(t), Z(t)) \geq 0$ and conditions H_1 and H_2 are satisfied. Therefore, Γ_0 is globally asymptotically stable for $R_0^B < 1$. □

Epidemiologically, this means that when the model is given a small pertubation through the introduction of few infected individuals into the population, the solutions of the model will converge to the DFE whenever $R_0^B < 1$.

4.8 The Endemic Equilibrium

4.8.1 Existence of the Endemic Equilibrium

Theorem 4.8.1. *EVD is persistent in the population if $S^*(t), E^*(t)$ and $I^*(t)$ exists for all $t > 0$ whenever $R_0^B > 1$.*

Proof. The positive endemic equilibrium (EE) of model (4.1) is given by

$$\Gamma^* = (S^*, E^*, I^*) \tag{4.14}$$

To get Γ^*, we equate the right hand side of each equation of model (4.1) to zero and then we solve explicitly using elementary row operations.

This gives us the following results;

$$\begin{aligned} S^* &= \frac{(\mu+\sigma)(\omega+\psi+\mu)}{(1-qv)\lambda\sigma,} \\ &= \frac{\Lambda}{\mu R_0^B}, \\ E^* &= \frac{\Lambda - \frac{\Lambda}{R_0^B}}{\sigma+\mu,} \\ &= \frac{\Lambda(R_0^B-1)}{R_0^B(\sigma+\mu),} \\ I^* &= \frac{\sigma\Lambda(R_0^B-1)}{R_0^B(\mu+\sigma)(\omega+\psi+\mu)}, \\ &= \frac{\mu(R_0^B-1)}{(1-qv)\lambda}. \end{aligned} \tag{4.15}$$

The set of equations denoted by Equation (4.15) shows that $S^*, E^*, I^* > 0$ whenever $R_0^B > 1$. This shows that the Endemic Equilibrium point exists whenever $R_0^B > 1$. □

4.8.2 Local Stability Analysis of the Endemic Equilibrium

Theorem 4.8.2. *The EE point $\Gamma^* = (S^*, E^*, I^*)$ is locally asymptotically stable.*

Proof. The Jacobian matrix of model (4.1) is as given earlier by matrix (4.9).

Evaluating matrix (4.9) at Γ^*, we get

$$J(\Gamma^*) = \begin{pmatrix} -\mu R_0^B & 0 & \frac{-(1-qv)\lambda\Lambda}{R_0^B} \\ \mu(R_0^B-1) & -(\sigma+\mu) & \frac{(1-qv)\lambda\Lambda}{R_0^B} \\ 0 & \sigma & -(\omega+\psi+\mu) \end{pmatrix} \tag{4.16}$$

The nature of the eigenvalues of matrix (4.16) gives us insights into the local stability of EE. We therefore compute these eigenvalues. This involves solving the equation

$$\begin{vmatrix} -\mu R_0^B - Z & 0 & \frac{-(1-qv)\lambda\Lambda}{R_0^B} \\ \mu(R_0^B-1) & -(\sigma+\mu)-Z & \frac{(1-qv)\lambda\Lambda}{R_0^B} \\ 0 & \sigma & -(\omega+\psi+\mu)-Z \end{vmatrix} = 0 \tag{4.17}$$

The characteristic equation (4.17) is given by

$$Z^3 + (\mu R_0^B + \sigma + \omega + \psi + 2\mu)Z^2 + \mu R_0^B(\sigma+\omega+\psi+2\mu)Z + \mu(R_0^B-1)(\sigma+\mu)(\omega+\psi+\mu) = 0 \tag{4.18}$$

which can be written as

$$Z^3 + CZ^2 + DZ + E = 0 \tag{4.19}$$

where

$$\begin{aligned} C &= (\mu R_0^B + \sigma + \omega + \psi + 2\mu), \\ D &= \mu R_0^B(\sigma + \omega + \psi + 2\mu), \\ E &= \mu(R_0^B - 1)(\sigma + \mu)(\omega + \psi + \mu). \end{aligned} \tag{4.20}$$

Using the Descartes' rule [50], the number of real roots of Equation (4.19) that are negative is equal to the number of changes in the signs of the coefficients of $f(-Z) = 0$ i.e $-Z^3 + CZ^2 - DZ + E = 0$.

The signs have changed 3 times hence the negative real roots are 3. Therefore each of the three eigenvalues of matrix (4.16) has a negative real part.

Thus, the EE of model (4.1) is locally asymptotically stable. □

This implies that if the system is pertubed by introducing few infected individuals, the solutions of the model will ultimately converge at the EE point whenever $R_0^B > 1$. Therefore, whenever $R_0^B > 1$, the disease will persist in the population.

4.8.3 Global Stability Analysis of the Endemic Equilibrium

The geometric approach proposed by Li. *et al* [25] is used in this subsection.

The Jacobian matrix of the model (4.1)is given by matrix (4.9). Writing matrix (4.9) as

$$J = \begin{pmatrix} J_{11} & J_{12} & J_{13} \\ J_{21} & J_{22} & J_{23} \\ J_{31} & J_{32} & J_{33} \end{pmatrix} \tag{4.21}$$

the second compound matrix corresponding to matrix (4.21) is given by

$$J^{[2]} = \begin{pmatrix} J_{11} + J_{22} & J_{23} & -J_{13} \\ J_{32} & J_{11} + J_{33} & J_{12} \\ -J_{31} & J_{21} & J_{22} + J_{33} \end{pmatrix} \tag{4.22}$$

$$J^{[2]} = \begin{pmatrix} -(1-qv)\lambda I(t) - B_1 & (1-qv)\lambda S(t) & (1-qv)\lambda S(t) \\ \sigma & -(1-qv)\lambda I(t) - B & 0 \\ 0 & (1-qv)\lambda I(t) & -\sigma - B \end{pmatrix} \tag{4.23}$$

where $B_1 = 2\mu + \sigma$ and $B = \omega + \psi + 2\mu$ Define an auxilliary matrix function A on the region Ω as

$$A = \begin{pmatrix} 1 & 0 & 0 \\ 0 & \frac{E(t)}{I(t)} & 0 \\ 0 & 0 & \frac{E(t)}{I(t)} \end{pmatrix} \tag{4.24}$$

This gives $A^{-1} = \begin{pmatrix} 1 & 0 & 0 \\ 0 & \frac{I(t)}{E(t)} & 0 \\ 0 & 0 & \frac{I(t)}{E(t)} \end{pmatrix}$.
Since $E(t), I(t) > 0$ everywhere in Ω, A is smooth and nonsingular.

Furthermore, we find that

$$A_f = \begin{pmatrix} 0 & 0 & 0 \\ 0 & \frac{E^{'}(t)I(t) - I^{'}(t)E(t)}{I^2(t)} & 0 \\ 0 & 0 & \frac{E^{'}(t)I(t) - I^{'}(t)E(t)}{I^2(t)} \end{pmatrix} \tag{4.25}$$

and

$$A_f A^{-1} = \begin{pmatrix} 0 & 0 & 0 \\ 0 & \frac{E^{'}(t)}{E(t)} - \frac{I^{'}(t)}{I(t)} & 0 \\ 0 & 0 & \frac{E^{'}(t)}{E(t)} - \frac{I^{'}(t)}{I(t)} \end{pmatrix} \tag{4.26}$$

Now

$$AJ^{[2]} = \begin{pmatrix} -(1-qv)\lambda I(t) - B_1 & (1-qv)\lambda S(t) & (1-qv)\lambda S(t) \\ \frac{\sigma E(t)}{I(t)} & \frac{\left[-(1-qv)\lambda I(t) - B\right]E(t)}{I(t)} & 0 \\ 0 & (1-qv)\lambda E(t) & \frac{(-\sigma - B)E(t)}{I(t)} \end{pmatrix} \tag{4.27}$$

Thus

$$AJ^{[2]}A^{-1} = \begin{pmatrix} -(1-qv)\lambda I(t) - B_1 & \frac{(1-qv)\lambda S(t)I(t)}{E(t)} & \frac{(1-qv)\lambda S(t)I(t)}{E(t)} \\ \frac{\sigma E(t)}{I(t)} & -(1-qv)\lambda I(t) - B & 0 \\ 0 & (1-qv)\lambda I(t) & -\sigma - B \end{pmatrix} \tag{4.28}$$

Let the matrix $M = A_f A^{-1} + AJ^{[2]}A^{-1}$, i.e Equation (4.26)+ Equation (4.28).

Therefore, the matrix M is
$\begin{pmatrix} -(1-qv)\lambda I(t) - B_1 & \frac{(1-qv)\lambda S(t)I(t)}{E(t)} & \frac{(1-qv)\lambda S(t)I(t)}{E(t)} \\ \frac{\sigma E(t)}{I(t)} & \frac{E^{'}(t)}{E(t)} - \frac{I^{'}(t)}{I(t)} - (1-qv)\lambda I(t) - B & 0 \\ 0 & (1-qv)\lambda I(t) & \frac{E^{'}(t)}{E(t)} - \frac{I^{'}(t)}{I(t)} - \sigma - B \end{pmatrix}$.
Equivalently, matrix M can be written as $\begin{pmatrix} M_{11} & M_{12} \\ M_{21} & M_{22} \end{pmatrix}$ where

$$M_{11} = -(1-qv)\lambda I(t) - B_1,$$

$$M_{12} = \begin{pmatrix} \frac{(1-qv)\lambda S(t)I(t)}{E(t)} & \frac{(1-qv)\lambda S(t)I(t)}{E(t)} \end{pmatrix}$$

$$M_{21} = \begin{pmatrix} \frac{\sigma E(t)}{I(t)} \\ 0 \end{pmatrix} \tag{4.29}$$

and $M_{22} = \begin{pmatrix} \frac{E^{'}(t)}{E(t)} - \frac{I^{'}(t)}{I(t)} - (1-qv)\lambda I(t) - 2\mu - \omega - \psi & 0 \\ (1-qv)\lambda I(t) & \frac{E^{'}(t)}{E(t)} - \frac{I^{'}(t)}{I(t)} - \sigma - 2\mu - \omega - \psi \end{pmatrix}$

Let (u, v, w) denote a vector in $\mathbb{R}^3$ whose norm is given by $\|(u, v, w)\| = max\{|u|, |v|+|w|\}$.

Let $\mu(M)$ be a Lozinskii measure with respect to this norm.

We choose $\mu(M) \leq sup\{g_1, g_2\}$ where $g_1 = \mu_1(M_{11}) + |M_{12}|$ and $g_2 = \mu_1(M_{22}) + |M_{21}|$. Here, $|M_{12}|$ and $|M_{21}|$ are matrix norms and μ_1 denotes the Lozinskii measure, all with respect to l_1 vector norm.

$|M_{12}|$ and $|M_{21}|$ are given by $\frac{(1-qv)\lambda S(t)I(t)}{E(t)}$ and $\frac{\sigma E(t)}{I(t)}$ respectively.

Next, we calculate $\mu_1(M_{22})$ by taking the nondiagonal elements of each column of matrix (M_{22}) in absolute value and then add to the corresponding columns of the diagonal elements. This gives

$$M_{22}^{'} = \begin{pmatrix} \frac{E^{'}(t)}{E(t)} - \frac{I^{'}(t)}{I(t)} - 2\mu - \omega - \psi & 0 \\ (1-qv)\lambda I(t) & \frac{E^{'}(t)}{E(t)} - \frac{I^{'}(t)}{I(t)} - \sigma - 2\mu - \omega - \psi \end{pmatrix} \tag{4.30}$$

The spectral radius of $M_{22}^{'}$ is given by

$$\mu_1(M_{22}) = max\left(\frac{E^{'}(t)}{E(t)} - \frac{I^{'}(t)}{I(t)} - 2\mu - \omega - \psi, \frac{E^{'}(t)}{E(t)} - \frac{I^{'}(t)}{I(t)} - \sigma - \omega - \psi - 2\mu \right) \tag{4.31}$$

which is

$$\mu_1(M_{22}) = \frac{E^{'}(t)}{E(t)} - \frac{I^{'}(t)}{I(t)} - 2\mu - \omega - \psi \tag{4.32}$$

Therefore,

$$g_1 = -(1-qv)\lambda I(t) - 2\mu - \sigma + \frac{(1-qv)\lambda S(t)I(t)}{E(t)} \tag{4.33}$$

and

$$g_2 = \frac{E^{'}(t)}{E(t)} - \frac{I^{'}(t)}{I(t)} - 2\mu - \omega - \psi + \frac{\sigma E(t)}{I(t)} \tag{4.34}$$

From model (4.1) ,

$$\frac{E^{'}(t)}{E(t)} = \frac{(1-v)\lambda S(t)I(t)}{E(t)} + \frac{(1-q)v\lambda S(t)I(t)}{E(t)} - \sigma - \mu \tag{4.35}$$

and

$$\frac{I^{'}(t)}{I(t)} = \frac{\sigma E(t)}{I(t)} - \psi - \omega - \mu \tag{4.36}$$

Therefore we have

$$g_1 = \frac{E^{'}(t)}{E(t)} - (1-qv)\lambda I(t) - \mu \tag{4.37}$$

and

$$g_2 = \frac{E^{'}(t)}{E(t)} - \mu \tag{4.38}$$

Now,

$$\mu(M) \leq sup[g_1, g_2] = \Big[\frac{E^{'}(t)}{E(t)} - (1-qv)\lambda I(t) - \mu, \frac{E^{'}(t)}{E(t)} - \mu\Big] \tag{4.39}$$

This gives the inequality

$$\mu(M) \leq \frac{E^{'}(t)}{E(t)} - \mu \tag{4.40}$$

which on integration yields

$$\frac{1}{t}\int \mu(M)ds \leq \frac{1}{t}\ln\frac{E(t)}{E(0)} - \mu \tag{4.41}$$

$$\limsup_{t\to\infty} \frac{1}{t}\int \mu(M)ds < -\mu < 0 \tag{4.42}$$

Hence, the EE is globally asymptotically stable.

In epidemiology, this means that there is persistent spread of EVD in the population whenever $R_0^B > 1$.

4.9 Numerical Simulation and Discussion

In this section, MATLAB software is used to perform numerical simulation of model (4.1). The results are as given by Figure 4.2 to Figure 4.5 below.

Table 4.2: Parameter Estimates for the Model

Parameter	Description	units	Value	source
Λ	The rate of recruitment of the susceptibles.	$peopleperday$	0.6321	[29]
λ	The rate of infection.	day^{-1}	0.05	varies
q	Efficacy of vaccine		$(0 \leq q \leq 1)$	varies
μ	The natural mortality rate.	day^{-1}	0.0099	[6]
v	Rate of vaccination		$(0 \leq v \leq 1)$	varies
σ	Rate of development of symptoms	day^{-1}	0.083	[34]
ω	Rate of Recovery from EVD.	day^{-1}	0.1	[13]
ψ	Mortality rate induced by EVD.	day^{-1}	0.2	Assumed

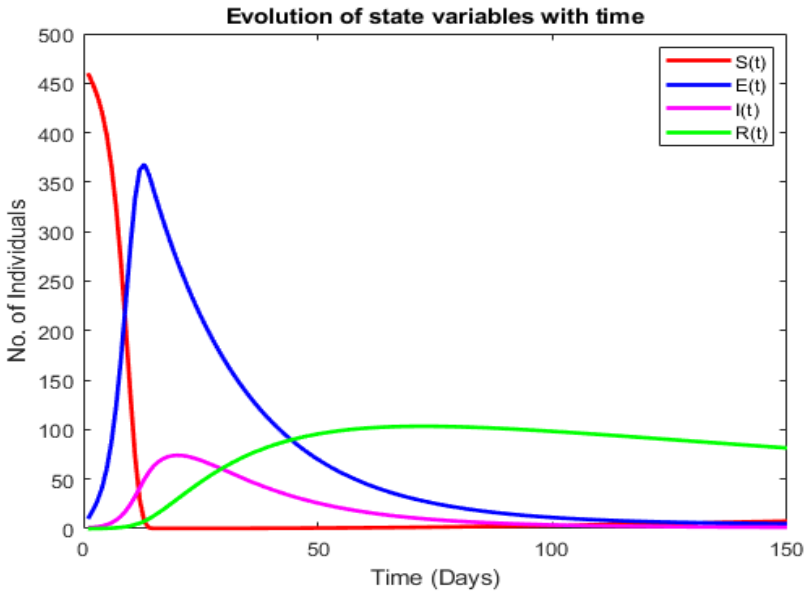

Figure 4.2: Evolution of State variables without intervention

The state variables evolve with respect to time as illustrated in Figure 4.2. One can see that as time increases, the number of individuals who are susceptible to EVD infection decreases. This is due to the fact that some of them get exposed and infected with EVD. The number of exposed, infected and recovered individuals increases up to particular levels then begin to decline. The increase is attributed to the numbers flowing from the susceptibles into the other classes.

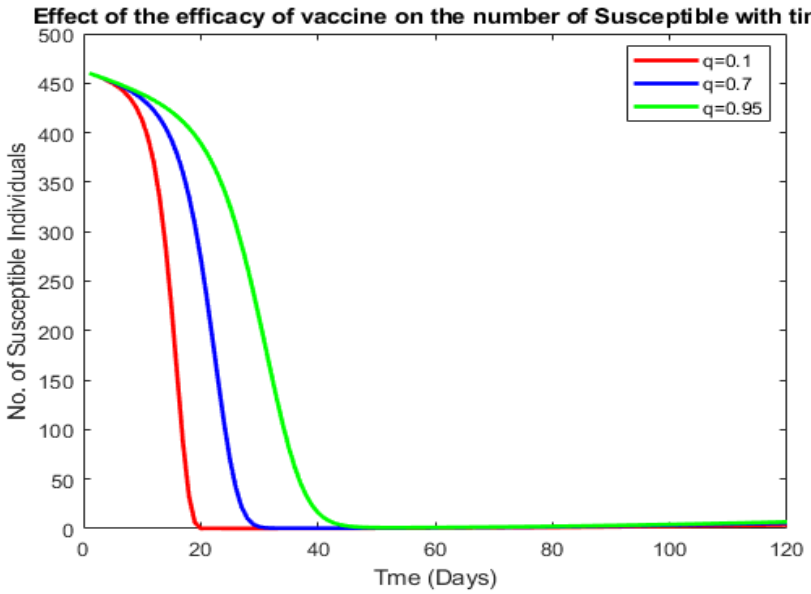

Figure 4.3: Evolution of Susceptible Individuals with varying efficacy of vaccine

From Figure 4.3, the number of susceptible individuals decreases rapidly when the efficacy of vaccination is low compared to when the efficacy is higher.

A vaccine makes the body to produce antibodies that fight the antigens. Therefore, when the vaccine is more effective, the body's immune system is more likely to subdue the infection than when the efficacy is low.

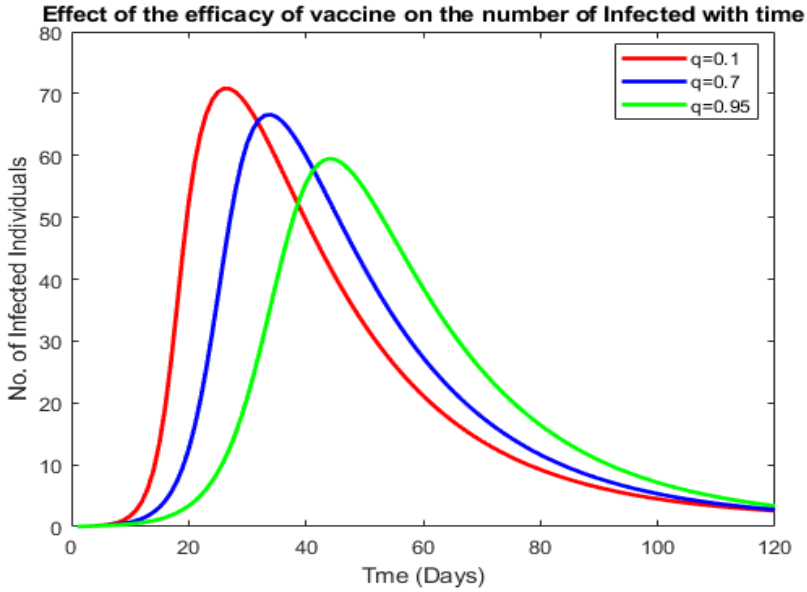

Figure 4.4: Evolution of Infected Individuals with varying efficacy of vaccine

When the efficacy of vaccine is low (e.g 10%), those who are infected increases rapidly in number from the first day until they reach a peak of 70 people on day 25. This is depicted in Figure 4.4. However, when it is 95%, the number of Infected individuals still rises but at a slower rate to reach a peak of about 58 people in the first 50 days. This shows that the efficacy of a vaccine plays a role in substantively affecting the number of infected individuals.

From the foregoing results, it can be seen that vaccination is an effective control strategy which can be considered to combat the deadly EVD, provided the efficacy of the vaccine is high.

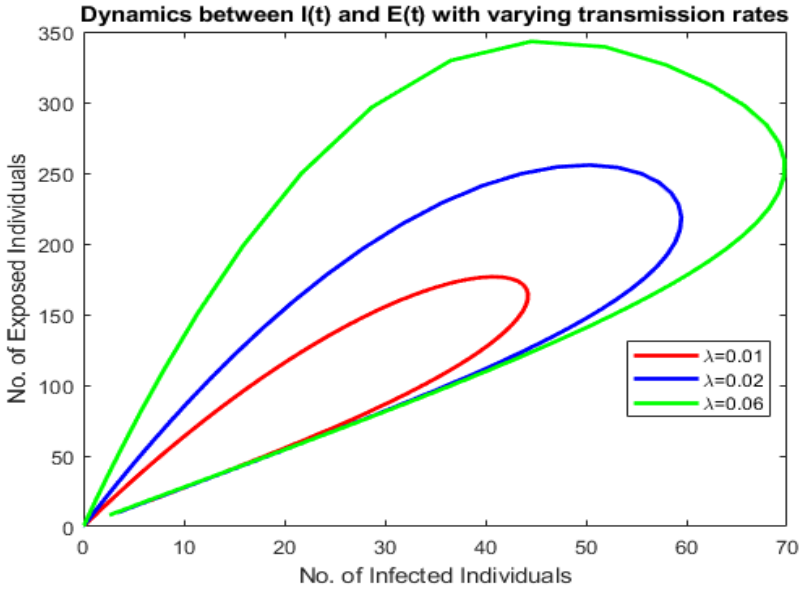

Figure 4.5: Dynamics between Infected and Exposed individuals

The relationship between the number of infected and exposed individuals is depicted by Figure 4.5. The two variables are directly proportional to each other since the infected individuals interact with the susceptibles to produce the exposed individuals. Therefore, when you increase the number of individuals who are infected with EVD, the number of susceptibles who come into contact with them also increases and this in turn increases the number of individuals exposed to the disease. From the graph, it can be seen that when the transmission rate is higher, the number of infected increases to a maximum of about 70 individuals and the corresponding exposed individuals are about 340. When the efficacy of vaccination is higher, transmission rate is lower since the body is able to fight and neutralise the invading pathogens. This leads to a lower number of infected individuals and the corresponding exposed individuals.

CHAPTER FIVE

MULTISCALE EBOLA MODEL

5.1 Introduction

Single scale models describing dynamics of diseases exist. Despite these extensive studies, the outbreak of some diseases, (including EVD) cannot still be predicted. This unpredictability may be attributed to the fact that these models are single scale yet disease dynamics are multiscale in nature. In the recent past, efforts have been directed towards multiscale models linking these two separate scales. The motivating factor in these efforts is the fact that there exists an interdependence of parameters between the different scales of infection. In this chapter, we develop and analyse a multiscale model of EVD derived from the within host model and between host model developed in chapters three and four respectively.

5.2 Within Host Model

The within host is given by

$$\begin{aligned} \frac{dX(t)}{dt} &= mX(t)(1-\frac{X(t)}{Q}) - (1-\rho)\beta\frac{L(t)X(t)}{1+kL(t)} - \alpha X(t), \\ \frac{dY(t)}{dt} &= (1-\rho)\beta\frac{L(t)X(t)}{1+kL(t)} - \eta Y(t), \\ \frac{dL}{dt} &= cY(t) - \gamma L(t) \end{aligned} \tag{5.1}$$

where the parameters and variables are as defined in chapter three.

5.3 Between Host Model

The between host model is given below

$$\begin{aligned}
\frac{dS(t)}{dt} &= \Lambda - (1-v)\lambda S(t)I(t) - (1-q)v\lambda S(t)I(t) - \mu S(t), \\
\frac{dE(t)}{dt} &= (1-v)\lambda S(t)I(t) + (1-q)v\lambda S(t)I(t) - \sigma E(t) - \mu E(t), \\
\frac{dI(t)}{dt} &= \sigma E(t) - (\omega + \psi + \mu)I(t), \\
\frac{dR(t)}{dt} &= \omega I(t) - \mu R(t)
\end{aligned} \tag{5.2}$$

where the parameters and variables are as defined in chapter four.

5.4 Multiscale Model

The multiscale model is developed by nesting the within host model into the between host model using the viral load of the within host model at equilibrium. This is presented graphically below

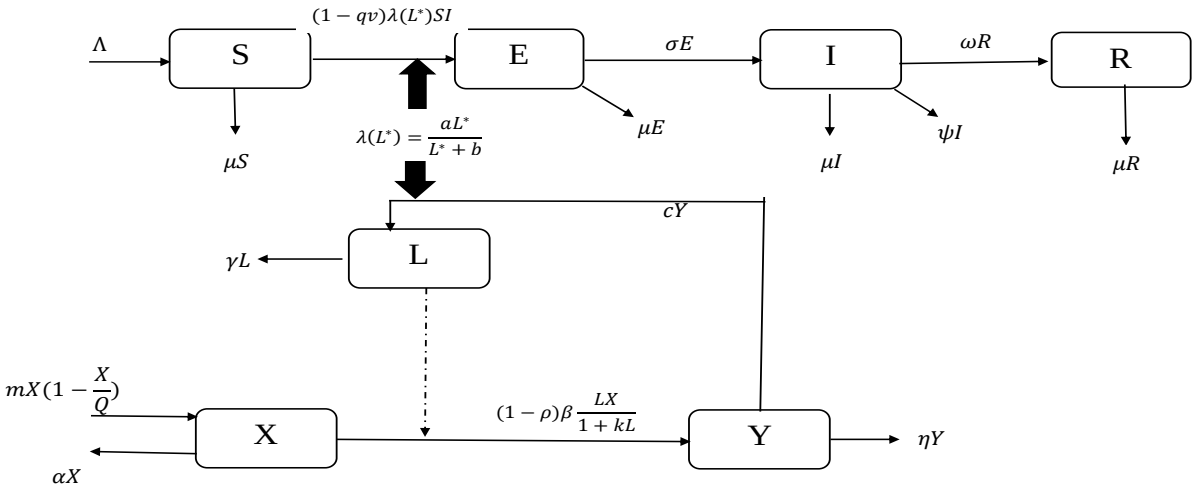

Figure 5.1: Flow Diagram of the Multiscale Model

These dynamics are represented mathematically by the system of ODEs below

$$\begin{aligned}
\frac{dS(t)}{dt} &= \Lambda - (1-v)\lambda(L^*)S(t)I(t) - (1-q)v\lambda(L^*)S(t)I(t) - \mu S(t), \\
\frac{dE(t)}{dt} &= (1-v)\lambda(L^*)S(t)I(t) + (1-q)v\lambda(L^*)S(t)I(t) - \sigma E(t) - \mu E(t), \\
\frac{dI(t)}{dt} &= \sigma E(t) - (\omega + \psi + \mu)I(t), \\
\frac{dR(t)}{dt} &= \omega I(t) - \mu R(t)
\end{aligned} \tag{5.3}$$

where $\lambda(L^*)$ is the transmission rate and is assumed to be an increasing function of L^* with $\lambda(0) = 0$ and L^* denotes the viral load at the endemic equilibrium in a single infected host. Here, $\lambda(L^*) = \frac{aL^*}{L^*+b}$ and $L^* = \frac{1}{k}[R_0^w - 1]$

It can be shown that model (5.3) is mathematically and epidemiologically well posed in the region $\Omega = \left\{ \Big(S(t), E(t), I(t), R(t) \Big) \in \mathbb{R}_+^4 | 0 < N(t) < \frac{\Lambda}{\mu} \right\}$ and therefore it suffices to consider it dynamically in this region.

In the model (5.3), the equation of the removed class is decoupled from the other three equations (since the recovered individuals are not able to spread the disease) and so we analyse the reduced model consisting of the first three equations. That is

$$\begin{aligned}
\frac{dS(t)}{dt} &= \Lambda - (1-qv)\lambda(L^*)S(t)I(t) - \mu S(t), \\
\frac{dE(t)}{dt} &= (1-qv)\lambda(L^*)S(t)I(t) - \sigma E(t) - \mu E(t), \\
\frac{dI(t)}{dt} &= \sigma E(t) - (\omega + \psi + \mu)I(t)
\end{aligned} \tag{5.4}$$

5.5 Reproduction number

The reproduction number for the coupled model (5.4), R_0^c is given by $\rho(FV^{-1})$ as described in [12]. Therefore,

$$R_0^c = \frac{(1-qv)\lambda(L^*)\Lambda\sigma}{\mu(\sigma+\mu)(\omega+\psi+\mu)} \tag{5.5}$$

5.6 Local Stability Analysis of the Disease Free Equilibrium

This is analysed using the theorem below.

Theorem 5.6.1. *If $R_0^c < 1$, then the DFE, $Z_0 = \left[\frac{\Lambda}{\mu}, 0, 0\right]$ is locally asymptotically stable.*

Proof. The Jacobian matrix of model (5.4) is given by

$$J = \begin{pmatrix} -(1-qv)\lambda(L^*)I(t) - \mu & 0 & -(1-qv)\lambda(L^*)S(t) \\ (1-qv)\lambda(L^*)I(t) & -\sigma - \mu & (1-qv)\lambda(L^*)S(t) \\ 0 & \sigma & -(\omega + \psi + \mu) \end{pmatrix} \tag{5.6}$$

Evaluating matrix (5.6) at the DFE, we obtain;

$$J(Z_0) = \begin{pmatrix} -\mu & 0 & \frac{-(1-qv)\lambda(L^*)\Lambda}{\mu} \\ 0 & -\sigma - \mu & \frac{(1-qv)\lambda(L^*)\Lambda}{\mu} \\ 0 & \sigma & -(\omega + \psi + \mu) \end{pmatrix} \tag{5.7}$$

The eigenvalues of matrix (5.7) gives insights into the stability of the DFE. We therefore compute these eigenvalues.

One of them is given by $-\mu$. To determine the nature of the remaining eigenvalues, the following reduced matrix is considered;

$$J_R = \begin{pmatrix} -\sigma - \mu & \frac{(1-qv)\lambda(L^*)\Lambda}{\mu} \\ \sigma & -(\omega + \psi + \mu) \end{pmatrix} \tag{5.8}$$

The trace of the matrix (5.8) is $-\sigma - \mu - (\omega + \psi + \mu)$ and it is negative.

The determinant of matrix (5.8) is given by

$$DetJ_R = (\sigma + \mu)(\omega + \psi + \mu) - \frac{(1-qv)\lambda(L^*)\Lambda\sigma}{\mu} \tag{5.9}$$

This determinant is positive if and only if

$\frac{(1-qv)\lambda(L^*)\Lambda\sigma}{\mu} < (\sigma + \mu)(\omega + \psi + \mu)$ i.e if $\frac{(1-qv)\lambda(L^*)\Lambda\sigma}{\mu(\sigma+\mu)(\omega+\psi+\mu)} < 1$

Meaning that the determinant is always positive whenever $R_0^c < 1$.

The Routh Hurwitz criterion of a negative trace and a nonnegative determinant which guarantee the existence of eigenvalues with negative real part has been met. Hence, the DFE is locally asymptotically stable whenever $R_0^c < 1$. □

5.7 Global Stability Analysis of the Disease Free Equilibrium

We use Comparison method [19] to analyse the global stability of the DFE as follows. At the Equilibrium point, $S(t) = N(t) - E(t) - I(t)$ and using the comparison theorem, we have

$$\begin{pmatrix} \frac{dE(t)}{dt} \\ \frac{dI(t)}{dt} \end{pmatrix} = (F - V) \begin{pmatrix} E(t) \\ I(t) \end{pmatrix} - \left(1 - \frac{\mu}{\Lambda} S(t)\right) \begin{pmatrix} 0 & (1 - qv)\lambda(L^*)S_0 \\ 0 & 0 \end{pmatrix} \begin{pmatrix} E(t) \\ I(t) \end{pmatrix} \quad (5.10)$$

Here, F and V are the Jacobian matrices for transmission and transition given respectively by

$$\begin{aligned} F &= \begin{pmatrix} 0 & \frac{(1-qv)\lambda(L^*)\Lambda}{\mu} \\ 0 & 0 \end{pmatrix} \text{ and} \\ V &= \begin{pmatrix} \sigma + \mu & 0 \\ -\sigma & \omega + \psi + \mu \end{pmatrix} \end{aligned} \quad (5.11)$$

so that

$$F - V = \begin{pmatrix} -\sigma - \mu & \frac{(1-qv)\lambda(L^*)\Lambda}{\mu} \\ \sigma & -(\omega + \psi + \mu) \end{pmatrix} \quad (5.12)$$

Equation (5.10) gives rise to the inequality

$$\begin{pmatrix} \frac{dE(t)}{dt} \\ \frac{dI(t)}{dt} \end{pmatrix} \leq (F - V) \begin{pmatrix} E(t) \\ I(t) \end{pmatrix} \quad (5.13)$$

Note that $(F-V)$ is equivalent to matrix (5.8) and so its eigenvalues have real parts which are negative. Therefore, the model (5.4) is stable whenever $R_0^c < 1$.

So $(E(t), I(t)) \to (0, 0)$ and $S(t) \to \frac{\Lambda}{\mu}$ as $t \to \infty$.

Using comparison theorem [19], $(S(t), E(t), I(t)) \to Z_0$ as $t \to \infty$.

Hence, Z_0 is globally asymptotically stable.

5.8 Existence of the Endemic Equilibrium

Theorem 5.8.1. *A positive endemic equilibrium point Z^* of model (5.4) exists for all time $t > 0$ provided $R_0^c > 1$*

Proof. The positive endemic equilibrium of model (5.4) is given by

$$Z^* = (S^*, E^*, I^*) \quad (5.14)$$

To get Z^*, we equate the right hand side of each equation of model (5.4) to zero and solve for the state variables explicitly using row operations. This gives the following results;

$$\begin{aligned} S^* &= \frac{(\mu+\sigma)(\omega+\psi+\mu)}{(1-qv)\lambda(L^*)\sigma,} \\ &= \frac{\Lambda}{\mu R_0^c}, \\ E^* &= \frac{\Lambda - \frac{\Lambda}{R_0^c}}{\sigma+\mu,} \\ &= \frac{\Lambda(R_0^c-1)}{R_0^c(\sigma+\mu),} \\ I^* &= \frac{\sigma\Lambda(R_0^c-1)}{R_0^c(\mu+\sigma)(\omega+\psi+\mu)}, \\ &= \frac{\mu(R_0^c-1)}{(1-qv)\lambda(L^*)}. \end{aligned} \tag{5.15}$$

Clearly from Equation (5.15), $E^* > 0$ and $I^* > 0$ provided $R_0^c > 1$. This ends the proof. □

5.9 Local Stability Analysis of the Endemic Equilibrium

This is investigated using the theorem below.

Theorem 5.9.1. *The Ebola Endemic Equilibrium point $Z^* = (S^*, E^*, I^*)$ is locally asymptotically stable if and only if the corresponding Jacobian matrix, $J(Z^*)$ is stable.*

Proof. The Jacobian matrix $J(Z^*)$ is given by

$$J(Z^*) = \begin{pmatrix} -(1-qv)\lambda(L^*)I^*(t) - \mu & 0 & -(1-qv)\lambda(L^*)S^*(t) \\ (1-qv)\lambda(L^*)I^*(t) & -\sigma-\mu & (1-qv)\lambda(L^*)S^*(t) \\ 0 & \sigma & -(\omega+\psi+\mu) \end{pmatrix} \tag{5.16}$$

Since all the diagonal elements of the matrix (5.16) are each less than zero and the fact that the eigenvalues of any square matrix are the same as those of its transpose, an argument using Gershgorin disks show that the matrix $J(Z^*)$ is stable if it is diagonally dorminant in columns [18]. Setting $\xi_1 = -\mu, \xi_2 = -\mu$ and $\xi_1 = -(\omega+\psi+\mu)$ gives

$$\xi = max[-\mu, -\mu, -(\omega+\psi+\mu)] < 0 \tag{5.17}$$

Equation (5.17) implies diagonal dorminance hence the proof. □

5.10 Global Stability Analysis of the Endemic Equilibrium

Theorem 5.10.1. *The endemic equilibrium point $Z^* = (S^*, E^*, I^*)$ is globally asymptotically stable.*

Proof. By making change of variables and using Lyapunov method, define the function

$$Y = M^{*2} + \Xi^{*2} + O^{*2} \tag{5.18}$$

where

$$\begin{aligned} M^* &= S - \frac{\Lambda}{(1-qv)\lambda(L^*)I + \mu}, \\ \Xi^* &= E - \frac{(1-qv)\lambda(L^*)SI}{\sigma + \mu}, \\ O^* &= I - \frac{\sigma E}{\omega + \psi + \mu} \end{aligned} \tag{5.19}$$

Considering equation(5.18), it is clear that $Y(0,0,0) = (0,0,0)$ and $Y(M^*, \Xi^*, O^*) > 0$ for all (M^*, Ξ^*, O^*) in the region Ω. In other words, Y is positive definite.

Differentiating Y with respect to time gives

$$\begin{aligned} \frac{dY}{dt} &= 2\Big[S - \frac{\Lambda}{(1-qv)\lambda(L^*)I + \mu}\Big]\Big(\frac{dS}{dt}\Big) + 2\Big[E - \frac{(1-qv)\lambda(L^*)SI}{\sigma + \mu}\Big]\Big(\frac{dE}{dt}\Big) \\ &+ 2\Big[I - \frac{\sigma E}{\omega + \psi + \mu}\Big]\Big(\frac{dI}{dt}\Big) \end{aligned} \tag{5.20}$$

where $\frac{dM^*}{dt} = \frac{dS}{dt}, \frac{d\Xi^*}{dt} = \frac{dE}{dt}, \frac{dO^*}{dt} = \frac{dI}{dt}$. Substituting the expressions for $\frac{dS}{dt}$, $\frac{dE}{dt}$ and $\frac{dI}{dt}$ from system (5.4) into equation (5.20) gives

$$\begin{aligned} \frac{dY}{dt} &= 2\Big[S - \frac{\Lambda}{(1-qv)\lambda(L^*)I + \mu}\Big]\Big(\Lambda - (1-qv)\lambda(L^*)SI - \mu S\Big) \\ &+ 2\Big[E - \frac{(1-qv)\lambda(L^*)SI}{\sigma + \mu}\Big]\Big((1-qv)\lambda(L^*)SI - \sigma E - \mu E\Big) \\ &+ 2\Big[I - \frac{\sigma E}{\omega + \psi + \mu}\Big]\Big(\sigma E - (\omega + \psi + \mu)I\Big) \end{aligned} \tag{5.21}$$

which is equivalent to

$$\begin{aligned} \frac{dY}{dt} &= -2\Big[S - \frac{\Lambda}{(1-qv)\lambda(L^*)I + \mu}\Big]^2\Big((1-qv)\lambda(L^*)I + \mu\Big) \\ &- 2\Big[E - \frac{(1-qv)\lambda(L^*)SI}{\sigma + \mu}\Big]^2\Big(\sigma + \mu\Big) \\ &- 2\Big[I - \frac{\sigma E}{\omega + \psi + \mu}\Big]^2\Big(\omega + \psi + \mu\Big) \end{aligned} \tag{5.22}$$

The right hand side of Equation (5.22) satisfies the conditions for a negative definite function. Therefore, $\frac{dY}{dt}$ is negative definite.

At the point Z^* given by equation (5.15),equation (5.22) becomes

$$\begin{aligned}\frac{dY}{dt} &= -2\Big[S^* - \frac{\Lambda}{(1-qv)\lambda(L^*)I^* + \mu}\Big]^2\Big((1-qv)\lambda(L^*)I^* + \mu\Big) \\ &- 2\Big[E^* - \frac{(1-qv)\lambda(L^*)S^*I^*}{\sigma+\mu}\Big]^2\Big(\sigma+\mu\Big) \\ &- 2\Big[I^* - \frac{\sigma E^*}{\omega+\psi+\mu}\Big]^2\Big(\omega+\psi+\mu\Big) \qquad (5.23)\end{aligned}$$

From equation (5.23), $\frac{dY}{dt} < 0$ since S^*, E^* and I^* are all greater than 0. Therefore, Z^* is globally asymptotically stable. □

5.11 Sensitivity Analysis

In this section, the sensitivity index of the reproduction number with respect to each parameter is obtained using the approach by Chitni [10] as follows.

$$\begin{aligned}\Gamma_{\Lambda}^{R_0^c} &= \frac{\partial R_0^c}{\partial \Lambda} \times \frac{\Lambda}{R_0^c} = 1 \\ \Gamma_{q}^{R_0^c} &= \frac{\partial R_0^c}{\partial q} \times \frac{q}{R_0^c} = \frac{-qv}{1-qv} \\ \Gamma_{\sigma}^{R_0^c} &= \frac{\partial R_0^c}{\partial \sigma} \times \frac{\sigma}{R_0^c} = \frac{\mu}{\sigma+\mu} \\ \Gamma_{v}^{R_0^c} &= \frac{\partial R_0^c}{\partial v} \times \frac{v}{R_0^c} = \frac{-qv}{1-qv} \\ \Gamma_{\psi}^{R_0^c} &= \frac{\partial R_0^c}{\partial \psi} \times \frac{\psi}{R_0^c} = -\omega(\omega+\psi+\mu) \\ \Gamma_{\omega}^{R_0^c} &= \frac{\partial R_0^c}{\partial \omega} \times \frac{\omega}{R_0^c} = -\omega(\omega+\psi+\mu) \\ \Gamma_{L^*}^{R_0^c} &= \frac{\partial R_0^c}{\partial L^*} \times \frac{L^*}{R_0^c} = \frac{b}{L^*+b}\end{aligned}$$

The sensitivity indices are given in Table 5.1.

Table 5.1: Sensitivity indices

Parameter	Value	Units	Sensitivity Index
Λ	0.6321	$peopleperday$	1
q	[0,1]		[0,-1.5]
μ	0.0099	day^{-1}	-1.13851199
v	[0,1]		[0,-1.5]
σ	0.083	day^{-1}	0.1065662
ω	0.1	day^{-1}	-0.03099
ψ	0.2	day^{-1}	-0.06198
L^*	8460.054	day^{-1}	0.011682169

From Table 5.1, it can be seen that the reproductive number R_0^c is directly proportional to the parameters σ and L^* in that increasing each one of them increases the reproduction number. On the other hand, q, μ, v, ω, and ψ are inversely proportional to R_0^c. These parameters are considered more sensitive as opposed to the parameters with positive sensitivity index. The most sensitive parameters are the efficacy of vaccination, q and the rate of vaccination, v. The sensitivity index of R_0^c with respect to q is -1.5 implying that increasing (or decreasing) q by 10% decreases (or increases)R_0^c by 15%. This means that the enhancement of the administration of an effective Ebola virus vaccine would reduce Ebola transmission in the population.

This agrees by the study which was done by Lawrence and Anne in [24] who through simulations, showed that vaccination effectively reduces the basic reproduction number of the model.

5.12 Numerical Simulation and Discussion

In this section, numerical simulation is done using the parameter values given in the Table 5.2 to explore model (5.4). The results are as given by Figure 5.2 to Figure 5.4.

Table 5.2: Values of the parameters in the model

Parameter	Relevant Biological Description	units	Value	source
a	Rate of transmission due to viral load	$Mlday^{-1}$	0.0025	[2]
b	Half saturation constant of virus	day^{-1}	100	[3]
Λ	Rate of recruitment	$peopleperday$	0.6321	[29]
λ	Transmission rate between hosts	day^{-1}	0.05	varies
q	Reduced Transmission rate		$(0 \leq q \leq 1)$	varies
μ	Natural death rate	day^{-1}	0.0099	[6]
v	Rate of vaccination		$(0 \leq v \leq 1)$	varies
σ	Rate of developing symptoms	day^{-1}	0.083	[34]
ω	Recovery rate	day^{-1}	[0.01,0.1,0.2]	[13]
ψ	Disease induced death rate	day^{-1}	0.2	Assumed

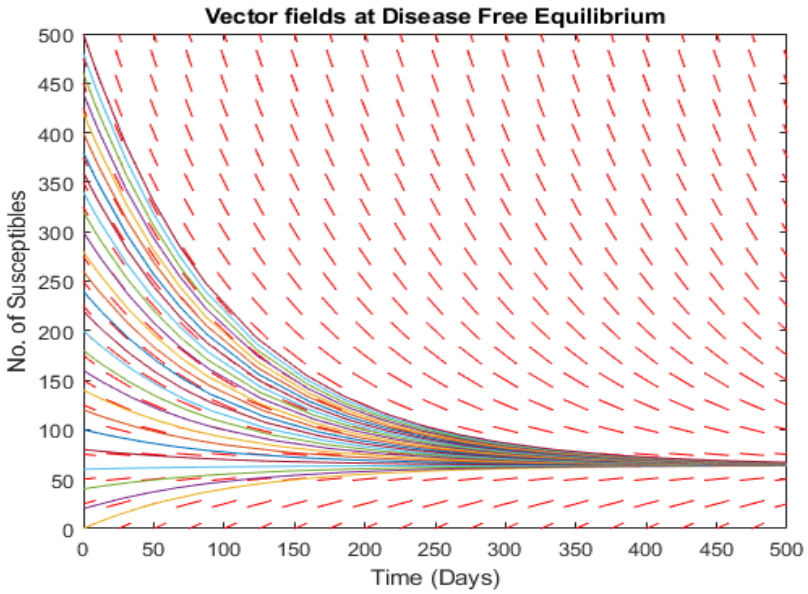

Figure 5.2: The stability of DFE

From these numerical simulations, the stability of the DFE is depicted by Figure 5.2. It can be seen that all the solutions are converging at the point $[63.85, 0, 0, 0]$ regardless of the starting point. This is the DFE point where $S_0 = \frac{\Lambda}{\mu} = 63.85$. This agrees with the analysis done above on the stability of the DFE.

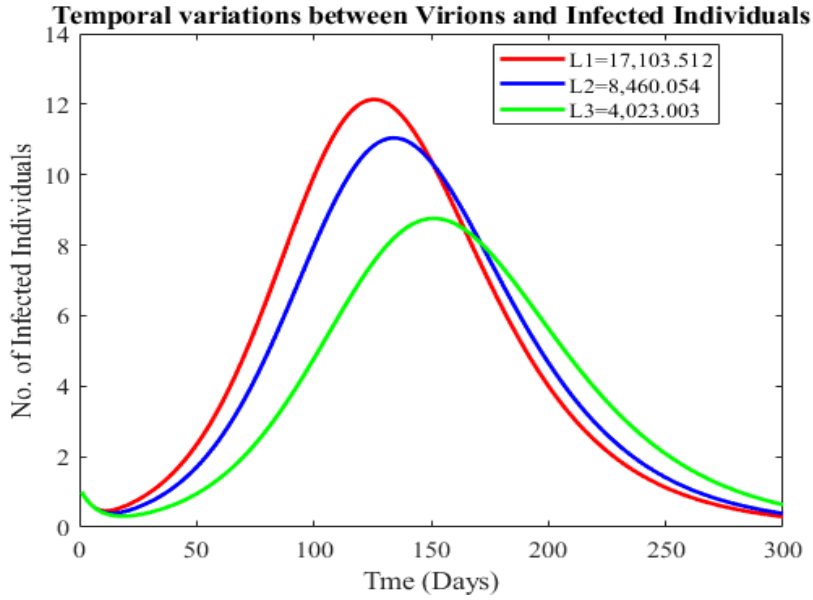

Figure 5.3: Effect of number of Virions on Infected individuals

Figure 5.3 depicts the effect of the coupling function, $\lambda(L^*)$ on the number of infected individuals. It can be seen that when L^* is bigger (meaning $\lambda(L^*)$ is also bigger since $\lambda(L^*)$ is an increasing function of L^*), the number of infected individuals increases. This increase can be attributed to the fact that as viral load within the individuals increases, there is a corresponding increase in the average viral load in the population and this affects the transmission of the disease positively. However, this increase in the number of individuals who are infected reaches a maximum point then begins to decrease. This decrease can be attributed to the recovery of the infected due to the effect of effective treatment, death of the infected individuals due to high viral load or susceptible individuals taking precautionary measures to prevent infection. This shows us that the viral load within an individual does affect the transmission dynamics of EVD between hosts. The variations in the viral load L^* used here were arrived at by varying the efficacy of treatment ρ. It was observed that the viral load L^* and the efficacy of treatment are inversely proportional to one another.

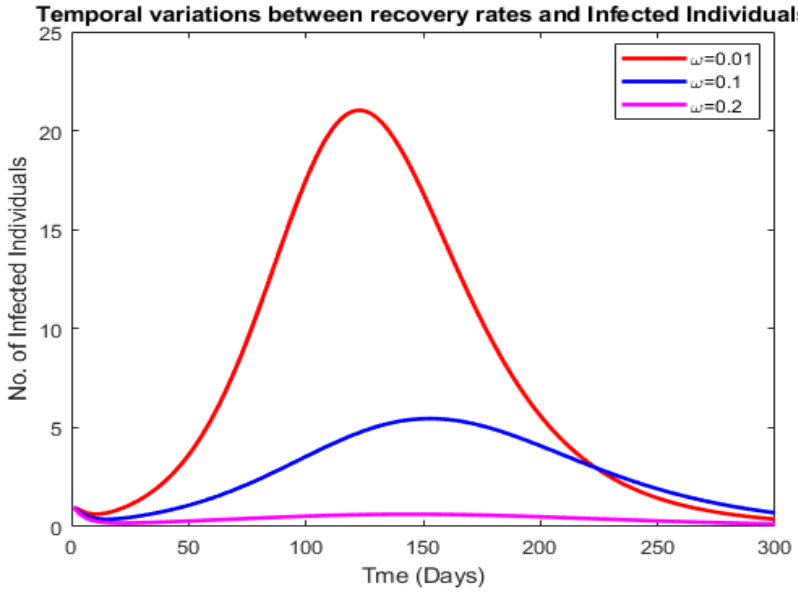

Figure 5.4: Effect of ω on Infected individuals with time

The relationship between recovery rates and the number of infected individuals is depicted in Figure 5.4. It can be seen that when the recovery rate is very low, the number of those who are infected peaks at a higher value than when the recovery rate is high. Efforts should be directed towards increasing the recovery rate of those already infected with EVD. One of the strategies to achieve this is treatment.

EVD is a highly infectious and deadly disease and therefore prudent measures should be taken to combat and if possible eradicate it. We see that effort should be focussed on identifying and treating the infected individuals and the efficacy of treatment should be higher so as to achieve higher recovery rates as has been illustrated by the simulations. It will also be prudent to put in place strategies to prevent the susceptible individuals from being exposed to the virus. One of these strategies is vaccination. The vaccine administered should be able to stimulate the body to produce antibodies within a short time since EVD causes hemorrhagic complications in a human being within a short time.

CHAPTER SIX

CONCLUSIONS AND RECOMMENDATIONS

6.1 Conclusions

This study aimed at developing and analysing a multiscale model for Ebola transmission dynamics with treatment. This has been achieved by developing and analysing three models as described below.

First, a within host model describing the Ebola transmission dynamics within an individual has been developed and analysed. The stability analysis of the results show that the IFE is both locally and globally stable. Center manifold Theorem has been used in the analysis to prove that the system has a unique EE that is stable. From numerical simulations, it can be concluded that the efficacy of treatment should be higher in order to tackle EVD. This is due to the fact that a higher efficacy of treatment makes the basic reproduction number to be < 1 and hence stifling new infections.

The second model is a between host SEIR model describing the dynamics of EVD. It has incorporated two parameters of vaccination i.e the rate of vaccination and the efficacy of vaccine. The DFE and the EE points of the model have been analysed and realized to be both locally and globally stable. The basic reproduction number was determined and proved that the disease is cleared from the population when $R_0^B < 1$ while it persists when $R_0^B > 1$. From the analysis and numerical simulations, it has been shown that with an imperfect vaccine, the disease can still be controlled.

Finally, we have derived a multiscale SEIR mathematical model describing EVD dynamics by coupling the between host model and the within host model using viral load. The basic reproduction number was determined and proved that the disease dies out when $R_0^c < 1$ and persists when $R_0^c > 1$. Numerical simulations focussing on the stability of the DFE, the effect of viral load (as a result of varying efficacy of treatment) and the effect of recovery rate ω on the number of infected individuals have been performed. Sensitivity analyses of the parameters has also been done. From the analysis and numerical simulations, it has been shown that viral load, which is a within host parameter affects the between host dynamics of EVD. These results are in agreement with the study conducted by Alexis E. S Almocera and Esteban A.H Vargas [2].

6.2 Recommendations

The following recommendations are made out of the results and simulations in this study;

(i) Based on our analysis and numerical simulations, we recommend that treatment of EVD should be done using drugs with high efficacy. This will go a long way in reducing the adverse effects of the disease in the population.

(ii) The multiscale model we have developed and analysed has considered a within host parameter affecting the between host dynamics of EVD. A study can be done on a parameter of between host model that affects the within host dynamics of EVD.

REFERENCES

[1] Aimee C., (2019, February 11) Congo's Ebola Outbreak is a testing ground for new treatments. *ScienceNews.* Retrieved from: https://www.sciencenews.org/article/congo-ebola-outbreak-testing-new-treatments.

[2] Alexis E.S.A., & Esteban A.H.V.,(2019). Coupling multiscale Within-host dynamics and Between-host transmission with recovery (SIR) dynamics *Mathematical Biosciences*, 309, 34-41. https://doi.org/10.1016/j.mbs.2019.01.001

[3] Alexis E.S.A.,Van K.N.,Esteban A.H.V.,(2018). Multiscale Model of Within-host and Between-host for Viral Infectious Diseases. *Journal of Mathematical Biology*, 77(4), 1035-1057. https://doi.org/10.1007/s00285-018-1241-y

[4] Amira R., & Delfim F.M.T, (2015). Mathematical Modelling, Simulation and Optimal Control of the 2014 Ebola Outbreak in West Africa. *Discrete Dyn. Nat. Soc* Art. ID 842792, 9 http://dx.doi.org/10.1155/2015/842792.

[5] Amira R., & Delfim F.M.T, (2015). Predicting and controlling the Ebola Infection. *Mathematical Methods in the Applied Sciences.*

[6] Amira R., & Delfim F.M.T, (2018). Analysis, Simulation and Optimal Control of a SEIR Model for Ebola Virus with Demographic Effects. *Commun. Fac. Sci.Univ. Ank. Ser. A1*, 67, 179-197.

[7] Castillo-Chavez C., Zhilan F., Wenzhan H., (2002). On the computation of R_0 and its role in global stability. In: Mathematical approaches for emerging and re emerging infectious diseases. *Institute for Mathematics and its Applications,* 67, 229-250.

[8] CDC(2016). 2014-2016 West African Outbreak: *Ebola survivors Questions and Answers.*

[9] (2019, November 5). Ebola Virus Disease Transmission. *Centers for Disease Control and Protection.* Retrieved from:https://www.cdc.gov/vhf/ebola/transmission/index.html

[10] Chitnis N., Hyman J., Cushing J., (2008). Residual viremia in treated HIV+ individuals Epidemiology, *Computational Biology.* 12, 597-677.

[11] David G.L., (1976). Introduction to Dynamical Systems. *John Wiley and Sons Inc.* U.S.A

[12] Dieckmann U., Metz J., Sabelis M., Sigmund K., (2002). Adaptive dynamics of infectious diseases: In pursuit of virulence management. *Cambridge University Press.* New York

[13] Durojaye M.O., & Ajie I.J., (2017). Mathematical Model of the Spread and Control of Ebola Virus Disease. Applied Mathematics, 7(2), 23-31. https://doi.org/10.5923/j.am.20170702.02

[14] (2019, August 14). Ebola Treatment trial: Two drugs identified as more effective. *European Centre for Disease Prevention and Control* . Retrieved from: https://www.ecdc.europa.eu/en/news-events/ebola-treatment-trial-two-drugs-identified-more-effective

[15] Ellina V.G., Evgenii K., (2015). Optimal Intervention Strategies for a SEIR control Model of Ebola Epidemics. *MDPI* ,3, 961-983.

[16] Feng Z.,Jorge V.,Brenda T., (2013). A mathematical model for coupling within-host and between-host dynamics in an environmentally-driven infectious disease.*Mathematical Biosciences*, 241, 4955.

[17] Heffernan J.M., Smith R.J., Wahi L.M., (2005). Perspectives on the basic reproductive ratio. *J. R. Soc. Interface* 2, 281-293. https://doi.org/10.1098/rsif.2005.0042

[18] Ibrahim M., Mugisha J., Mohsin H., (2010) Mathematical Analysis of the dynamics of Visceral leishmaniasis in the Sudan. *Applied Mathematics and Computation*, 217, 2567-2578

[19] James W., Van D., Further Notes on the Basic Reproduction Number. In: Brauer F., van den Driessche P., Wu J. (eds) Mathematical Epidemiology. Lecture Notes in Mathematic. vol 1945. *Springer*. Berlin.

[20] Jie L., Hongna L., Dong L.,Zhen J., Baojun S., (2015). The Coupled Within and Between-host Dynamics in the evolution of HIV/AIDS in China. *Journal of Applied Analysis and Computation* 5, 735-750.

[21] Kelly S., (2014, August 13). What Does Ebola actually do? *ScienceMag*. Retrieved from: https://www.sciencemag.org/news/2014/08/what-does-ebola-actually-do?intcmp=collection-ebola

[22] Lasisi N.O., Akinwande N.I., Olayiwola R.O., Cole A.T, (2018). Mathematical Model for Ebola Virus Infection in Human with Effectiveness of Drug Usage. *J. Appl. Sci. Environ. Manage.* 22 (7), 1089-1095.

[23] Lawi G.O., Mugisha J.Y.T., Omolo N.O., (2011). Mathematical Model for Malaria and Meningitis Co-infection among Children. *Applied Mathematical Sciences* 5(47), 2337 - 2359.

[24] Lawrence O., & Anne M., (2017). *Analysis of the Effect of Vaccination on Ebola Dynamics IJEIR* 6, 127-132.

[25] Li M.Y, Muldowney J.S., (1996). A Geometric Approach to global- stability problems. *Journal of Mathematical Analysis* 27(4), 1070-1083.

[26] Lucey D.R.,(2019). New Treatments for Ebola Virus Disease *BMJ* https://doi.org/10.1136/bmj.15371

[27] Maia M.,Necibe T.,Colette M., (2015). Coupling Within-host and Between-host infectious Diseases Models. *Biomath* 4, https://doi.org/10.11145/j.biomath.2015.10.091

[28] Mossong J., Hens N., Jit M., (2008) Social contacts and mixing patterns relevant to the spread of infectious diseases. *PLoS Med.* 5(3) https://doi.org/10.1371/journal.pmed.0050074

[29] Muhammad T.,Syed I.A.S, Gul Z., Sher M., (2018). Ebola virus epidemic disease its modeling and stability analysis required abstain strategies. *Cogent Biology* 4(1) https://doi.org/10.1080/23312025.2018.1488511

[30] Navjot K.,Mini G.,Bhatia S., (2014). Modeling and analysis of an SIRS Epidemic Model with Effect of Awareness Programs by Media. *IJMCPECE*, 8(1), 233- 239.

[31] Van N., Rafael M., Esteban A., (2017). Multiscale modeling to explore Ebola vaccination strategies. *bioRxiv*. http://dx.doi.org/10.1101/133421

[32] Nowak M.A. & May R.M. (2000). *Virus dynamics* Oxford University press, New York.

[33] Numfor E.,Bhattcharyn S.,Lenhart S.,Martcheva M., (2014). Optimal Control in Coupled Within-host and Between-host Models. *Math.Model.Nat.Phenom.* 9(4), 171-203. https://doi.org/10.1051/mmnp/20149411

[34] Oduro F.T.,George A., Joseph B.,(2016). Optimal Control of Ebola Transmission Dynamics with Interventions. *Science Domain International*. 19(1), 1-19.

[35] Perelson A.S., & Nelson P.W., (1999). Mathematical analysis of HIV-1 dynamics in vivo. *SIAM* 41, 3 - 44.

[36] Song X., Neumann A.U., (2007). Global stability and periodic solution of the viral dynamics. *J. Math. Anal. Appl.* 329, 281 297.

[37] Sophia B.,Zvi R.,Mirjana P., (2010). Mathematical Modeling of Ebola Virus Dynamics as a step towards Rational Vaccine Design. *IFMBE* 32, 196-200.

[38] Sylvie D.D.N.,(2015). *Modelling the potential role of control strategies on Ebola virus disease dynamics* (Masters Thesis, University of Stellenbosch.) Retrieved from http://www.scholar.sun.ac.za

[39] Thomas W., (2015). Analysis and Simulation of a Mathematical Model of Ebola Virus Dynamics in Vivo. *SIAM.*

[40] Thomas W., Boping T., Zunyou W., (2017). *Modeling the effect of quarantine and vaccination on Ebola disease*. Advances in Difference Equations. http://dx.doi.org/10.1186/s13662-017-1225-z

[41] Tomislav M., (2016). Retrieved from://www.news-medical.net/health/what-is-Ebola.aspv.

[42] Van den Driessche P., Watmough J. Reproduction numbers and sub-threshold endemic equilibria for compartmental models of disease transmission. *Mathematical Biosciences* 180, 29-48. http://doi.org/10.1016/s0025-5564(02)00108-6

[43] Vincent M., Lisa O.,Frederick G.,Thi H.,Tram N.,Xavier L.,France M.,Stephan G.,Jeremie G., (2015). Ebola Virus Dynamics in mice treated with favipiravir. *Antiviral Research.*123, 70-77. http://doi.org/10-1016/j.antiviral.2015.08.015.

[44] (2019, February 19) New Ebola Treatments are being tested in Congo Outbreak area. *Washington Post.* Retrieved from: https://www.washingtonpost.com/national/health-science/new-ebola-treatments-are-being-tested-in-congo-outbreak-area/2019/02/15/07d1b6fc-306c-11e9-813a-0ab2f17e305b story.html

[45] (2016, February 29) Ebola Virus Disease. *WHO.* Retrieved from: http://www.who.int/mediacenter/factsheet/fs103/en/.

[46] (2019, April 12) Preliminary results on the efficacy of rVSV-ZEBOV-GP Ebola vaccine using the ring vaccination strategy in the control of an Ebola outbreak in

the Democratic Republic of the Congo: an example of integration of research into epidemic response. *WHO*. Retrieved from: http://www.who.int/blueprint/priority-diseases/key-action/ebola-additional-documents/en/

[47] (2016, April 21) Mathematical modeling of infectious disease. *Wikipedia*. Retrieved from: http://www.en.m.wikipedia.org/wiki/Mathematical-modeling-of-infectious disease.

[48] Winston G.,Dephney M., Rendani N.,(2014). A mathematical modelling framework for linked within-host and between-host dynamics for infections with free-living pathogens in the environment. *Mathematical Biosciences* 256, 58-78 http://doi.org/10.1016/j.mbs.2014.08.004

[49] Xi H., Xiaodan S., Kunquan L., Jianhong W., (2016). Treatmentdonation-stockpile dynamics in ebola convalescent blood transfusion therapy. *Journal of Theoretical Biology*, 392, 53-61. http://doi.org/10.1016/j.jtbi.2015.11.031.

[50] Xiaoshen W., (2004). A Simple proof of Descartes Rule of Signs. *Amer. Math Monthly*, 111, 525-526.

[51] Zhilan F.,Jorge V.,Brenda T.,Maria C.,(2011). A model for Coupling Within-host and Between-host Dynamics in an infectious Disease. *Nonlinear Dyn.* 68, 401 - 411. http://doi.org/10.1007/s 11071-011-0291-0

0.1 Codes used in simulating within host model

T = 100; dt = 0.5; N = 4; m = 0.1; Q = 1500; rho =[0.1,0.4,0.7,0.95]; beta = 0.0027; k=0.001; alpha = 0.02; eta = 0.24; c= 2.4; gamma = 2;

x(1:N,1) = [1000, 1000,1000,1000]';

y(1:N,1) = [5,5,5,5]';

l(1:N,1) = [0.01,0.01,0.01,0.01]

for t = 1:T

for i =1:N

x(i,t+1) = x(i,t) + dt*(m*x(i,t).*(1-x(i,t)/Q)-(1-rho(i))*beta*l(i,t).*x(i,t)./(1+k*l(i,t))-alpha*x(i,t));

y(i,t+1) = y(i,t) + dt*((1-rho(i))*beta*l(i,t).*x(i,t)./(1+k*l(i,t))-eta*y(i,t));

l(i,t+1) = l(i,t) + dt*(c*y(i,t)-gamma*l(i,t));

plot(1:T, x(:,1:T),'Linewidth',2);

plot(1:T, l(:,1:T),'Linewidth',2);

plot(1:T, y(:,1:T),'Linewidth',2);

legend($\rho = 0.1(R_0^w = 14.58), \rho = 0.4(R_0^w = 9.72), \rho = 0.7(R_0^w = 4.86), \rho = 0.95(R_0^w = 0.81)$);

ylabel 'No. of Target cells';

ylabel 'No. of Virions';

ylabel 'No. of Infected cells';

xlabel 'Time (Days)';

title('Effect of varying treatment (ρ) on Target cells with time')

title('Effect of varying treatment (ρ) on Virions with time')

title('Effect of varying treatment (ρ) on Infected cells with time')

0.2 Direction fields of IFE

```
T = 200; dt = 0.5; a = 0.02; N = 3; m = 0.1; Q = 1500; rho =0.4; beta = 0.0027; k=0.001;
alpha = 0.02; eta = 0.24; c= 2.4; gamma = 2;
x = zeros(20,T);
y= zeros(20,T);
l = zeros(20,T);
x(:,1) = (100:100:20*100)';
y(:,1) = [0,0,0,0,0,0,0,0,0,0,0,0,0,0,0,0,0,0,0,0]';
l(:,1) = [0,0,0,0,0,0,0,0,0,0,0,0,0,0,0,0,0,0,0,0]';
f = @(t,y1) 0.1*y1.*(1-y1./1500)-0.02.*y1;
for t = 1:T
x(:,t+1) = x(:,t) + dt*(m*x(:,t).*(1-x(:,t)/Q)-(1-rho)*beta*l(:,t).*x(:,t)./(1+k*l(:,t))-alpha*x(:,t));
y(:,t+1) = y(:,t) + dt*((1-rho)*beta*l(:,t).*x(:,t)./(1+k*l(:,t))-eta*y(:,t));
l(:,t+1) = l(:,t) + dt*(c*y(:,t)-gamma*l(:,t));
end
dirfield(f,0:10:10*20,0:100:2000);
hold on
plot(1:T,x(:,1:T),'Linewidth',2);
axis([0 200 0 2000])
hold off
ylabel 'No. of Target cells';
xlabel 'Time (Days)';
title('Stability of the Infection Free Equilibrium')
```

0.3 Between host model

```
T = 150, 120; dt = 0.5; N = 1, 3; Lambda = 0.6321; lambda = [0.01, 0.02, 0.05, 0.06];
q=[0.1, 0.5, 0.7, 0.95]; mu = 0.0099; v = 0.5,0.8; sigma = 0.083; omega = 0.1; psi = 0.2;
S = zeros(N,T);
E = zeros(N,T);
I = zeros(N,T);
R = zeros(N,T);


    S(1:N,1) = [460,460,460]';
E(1:N,1) = [1,1,1]';
I(1:N,1) = [0,0,0]';
R(1:N,1)= [0,0,0]';
for t = 1:T
for i =1:N
S(i,t+1) = S(i,t) + dt*Lambda - dt*(1-q*v)*lambda(i).*S(i,t).*I(i,t) - mu*S(i,t)*dt;
E(i,t+1) = E(i,t) + dt*(1-q*v)*lambda(i).*S(i,t).*I(i,t)-sigma*E(i,t)*dt-mu*E(i,t)*dt;
I(i,t+1) = I(i,t) + dt*(sigma*E(i,t)-(omega+psi+mu)*I(i,t));
R(i,t+1) = R(i,t) + dt*(omega*I(i,t)-mu*R(i,t));
end
plot(1:T,S(1,1:T),'r',1:T,E(1,1:T),'b',1:T,I(1,1:T),'m',1:T,R(1,1:T),'g','Linewidth',2.0);
legend('S(t)','E(t)','I(t)','R(t)','Location','best');
ylabel 'No. of Individuals';
xlabel 'Time (Days)';
title('Evolution of state variables with time')
plot(1:T,S(1,1:T),'r',1:T,S(2,1:T),'b',1:T,S(3,1:T),'g','Linewidth',2.0);
legend('q=0.1','q=0.7','q=0.95','Location','best');
ylabel 'No. of Susceptible Individuals';
xlabel 'Tme (Days)';
```

title('Effect of the efficacy of vaccine on the number of Susceptible with time')

plot(1:T,I(1,1:T),'r',1:T,I(2,1:T),'b',1:T,I(3,1:T),'g','Linewidth',2.0);

legend('q=0.1','q=0.7','q=0.95','Location','best');

ylabel 'No. of Infected Individuals';

xlabel 'Time (Days)';

title('Effect of the efficacy of vaccine on the number of Infected with time')

plot(I(1,1:T),E(1,1:T),'r',I(2,1:T),E(2,1:T),'b',I(3,1:T),E(3,1:T),'g','Linewidth',2.0);

legend($'\lambda = 0.01'$,$' \lambda = 0.02'$,$' \lambda = 0.06'$,'Location','best');

ylabel 'No. of Exposed Individuals';

xlabel 'No. of Infected Individuals';

title('Dynamics between I(t) and E(t) with varying transmission rates')

0.4 Multiscale model

T = 300; dt = 0.5; a = 0.0025; b= 100; N = 3; m = 3; Q = 1500; rho =[0.1,0.6,0.8]; beta = 0.0027; k= 0.001; alpha = 0.02; eta = 0.24; c= 2.4; gamma = 2; Lambda = 0.6321; lambda = 0.05; q = 0.3; mu = 0.0099; v = 0.8; sigma = 0.083; omega = [0.01,0.1,0.2]; psi = 0.2;

x = zeros(N,T);

y= zeros(N,T);

l = zeros(N,T);

S = zeros(N,T);

E = zeros(N,T);

I = zeros(N,T);

R = zeros(N,T);

x(1:N,1) = [1000, 1000,1000]';

y(1:N,1) = [5,5,5]';

l(1:N,1) = [0.01,0.01,0.01]';

```
S(1:N,1) = [460,460,460]';
E(1:N,1) = [1,1,1]';
I(1:N,1) = [1,1,1]';
R(1:N,1)= [0,0,0]';
for t = 1:T
for i =1:N
x(i,t+1) = x(i,t) + dt*(m*x(i,t).*(1-x(i,t)/Q)-(1-rho(i))*beta*l(i,t).*x(i,t)./(1+k*l(i,t))-
alpha*x(i,t));
y(i,t+1) = y(i,t) + dt*((1-rho(i))*beta*l(i,t).*x(i,t)./(1+k*l(i,t))-eta*y(i,t));
l(i,t+1) = l(i,t) + dt*(c*y(i,t)-gamma*l(i,t));
S(i,t+1) = S(i,t) + dt*Lambda - dt*(1-q*v)*a*(l(i,t+1)./(l(i,t+1)+b)).*S(i,t).*I(i,t) - mu*S(i,t)*dt;
E(i,t+1) = E(i,t) + dt*(1-q*v)*a*(l(i,t+1)./(l(i,t+1)+b)).*S(i,t).*I(i,t)-sigma*E(i,t)*dt-
mu*E(i,t)*dt;
I(i,t+1) = I(i,t) + dt*(sigma*E(i,t)-(omega(i)+psi+mu)*I(i,t));
R(i,t+1) = R(i,t) + dt*(omega(i)*I(i,t)-mu*R(i,t));
end
end
plot(1:T,I(1,1:T),'r',1:T,I(2,1:T),'b',1:T,I(3,1:T),'g','Linewidth',2.0);
legend('L1=17,103.512','L2=8,460.054','L3=4,023.003','Location','best');
ylabel 'No. of Infected Individuals';
xlabel 'Tme (Days)';
title('Temporal variations between Virions and Infected Individuals')
plot(1:T,I(1,1:T),'r',1:T,I(2,1:T),'b',1:T,I(3,1:T),'m','Linewidth',2.0);
legend('ω = 0.01′,′ ω = 0.1′,′ ω = 0.2','Location','best');
ylabel 'No. of Infected Individuals';
xlabel 'Tme (Days)';
title('Temporal variations between recovery rates and Infected Individuals')
```